UNIVERSIDADE FEDERAL DE SANTA MARIA
CENTRO DE TECNOLOGIA
PROPRAMA DE PÓS-GRADUAÇÃO EM ENGENHARIA QUÍMICA

Dison Stracke Pfingsten Franco

MODIFICAÇÕES NA CASCA DE ARROZ PARA A ADSORÇÃO DE AZUL DE METILENO EM BATELADA E LEITO FIXO

Santa Maria, RS
2016

Dison Stracke Pfingsten Franco

MODIFICAÇÕES NA CASCA DE ARROZ PARA A ADSORÇÃO DE AZUL DE METILENO EM BATELADA E LEITO FIXO

Dissertação apresentada ao Curso de Mestrado do Programa de Pós-Graduação em Engenharia Química, da Universidade Federal de Santa Maria (UFSM, RS), como requisito parcial para obtenção do grau de **Mestre em Engenharia Química**.

Orientador: Prof. Dr. Guilherme Luiz Dotto

Co-orientador: Prof. Dr. Eduardo H. Tanabe

Santa Maria, RS

2016

Dison Stracke Pfingsten Franco

MODIFICAÇÕES NA CASCA DE ARROZ PARA A ADSORÇÃO DE AZUL DE METILENO EM BATELADA E LEITO FIXO

Dissertação apresentada ao Curso de Mestrado do Programa de Pós-Graduação em Engenharia Química, da Universidade Federal de Santa Maria (UFSM, RS), como requisito parcial para obtenção do grau de **Mestre em Engenharia Química**.

Aprovado em 12 de agosto de 2016

Prof. Guilherme Luiz Dotto, Dr. (UFSM)
(Presidente/Orientador)

Prof. Edson Luiz Foletto, Dr. (UFSM)

Prof. André Ricardo Felkl de Almeida, Dr. (UNIPAMPA)

Santa Maria, RS
2016

AGRADECIMENTOS

Primeiramente gostaria de agradecer pelo suporte de meu pai Gilberto Franco e minha mãe Anna Elizabeth Pfingsten, sem eles não seria possível vencer esta e todas outras etapas da minha vida.

Agradecer ao meu orientador/chefe/amigo Guilherme Dotto, a oportunidade que me destes de conviver contigo estes últimos dois anos, as conversas, conselhos e experiências tanto profissionais e pessoais jamais serão esquecidas.

Ao meu co-orientador Eduardo Tanabe que sempre esteve presente para compartilhar suas ideias para a pesquisa e experiência na docência.

Aos meus colegas de pós-graduação, que sempre estiveram ao meu lado para dar risadas, conversar sobre as pesquisas, dilemas da vida e aguentar o colega chato deles. Em especial para Jair Daniel Júnior que de um total desconhecido virou um grande amigo que não irei esquecer jamais, para as minhas amigas, Susanne Druzian, Letícia Côrtes, Priscila Molinares que sempre estiveram ao meu lado.

Um agradecimento muito especial e único a minha namorada/amiga/companheira Martha Dessbesell, está não existe palavras suficientes para dizer o quanto me ajudou nesta jornada e nas que irá me acompanhar, talvez a única palavra seja "*Bolá*". E junto quero agradecer meu sogro e minha sogra, Ênio e Ângela Dessbesell, por me adotarem em seu lar como se fosse seu filho.

À Química Mariana Bassaco do DEQ/UFSM, pelo apoio na realização das análises e companheirismo profissional.

Aos Professores André Felkl e Edson Foletto por serem banca e avaliarem meu trabalho.

Aos demais professores e funcionários do PPGEQ

A CAPES pelo apoio financeiro.

E a todos aqueles que me ajudaram de alguma forma a evoluir e crescer durante esta jornada

RESUMO

Neste trabalho foi o investigado o uso casca de arroz e suas modificações como adsorvente do corante azul de metileno, em operações descontinua (batelada) e continua (leito fixo). A casca de arroz foi modificada utilizando tratamentos alternativos como: a extração supercrítica com CO_2, ultrassom assistido e ataque com hidróxido de sódio. Estes materiais foram caracterizados através de espectroscopia no infravermelho por transformada de Fourier (FTIV), difração de raios-X (DRX), microscopia de varredura eletrônica (MEV) e espectroscopia de raios-X por dispersão em energia (EDS). Na adsorção em batelada, os modelos de Langmuir e Hill mostraram que a adsorção foi espontânea e que, para todos os adsorventes, a capacidade de adsorção aumentou conforme o aumento da temperatura. Para a adsorção em leito fixo foi realizada uma otimização e aplicação dos adsorventes no ponto ótimo. Foram aplicados os modelos dinâmicos (Thomas, tempo de serviço de leito, Yoon-Nelson) a fim de descrever a curva de ruptura. No geral foi possível constatar que os tratamentos utilizados melhoraram a capacidade de adsorção para ambas as operações. Para a batelada, verificou-se que a capacidade de adsorção foi na seguinte ordem: casca de arroz modificada com NaOH (65.0 ±0,4 mg g^{-1}) > Ultrassom (58.7±2,1 mg g^{-1}) > CO_2 supercrítico (56.4±0,6 mg g^{-1}) > casca de arroz *in natura* (52.2 ±1.3 mg g^{-1}). No leito fixo o mesmo comportamento foi encontrado. O tempo de ruptura foi de 109, 240, 155 e 385 min, para casca de arroz *in natura*, casca de arroz tratada ultrassom assistido, CO_2 supercrítico e NaOH respectivamente.

Palavras-chave: Adsorção, Batelada, Leito Fixo, Casca de arroz, Azul de metileno, Tratamentos alternativos.

ABSTRACT

In this work, rice husk and its modifications were investigated as methylene blue adsorbents, using discontinuous (batch) and continuous (fixed bed) adsorption operations. The rice husk was modified through alternative treatments like; supercritical extraction with CO_2, assisted ultrasound and sodium hydroxide attacks. The adsorbents were characterized through Fourier transform infrared spectroscopy (FTIR), x-ray diffraction (XRD), scanning electron microscopy (SEM) and energy dispersive x-ray spectroscopy (EDS). For the batch adsorption, Langmuir and Hill models were used to describe the isotherms. From the thermodynamic perspective the adsorption was spontaneous and the adsorption capacity increases with the temperature increase. The fixed bed adsorption was optimized and adsorbents were applied in the optimal condition, then dynamic models (Thomas, BDST, Yoon-Nelson) were fitted to the experimental data to represent the breakthrough curve. In general it was found that the treatments enhanced the adsorption capacity for both process. For the batch process a pattern indicating that the NaOH rice husk (65.0 ±0.4 mg g^{-1}) was superior to UA (58.7 ±2,1 mg g^{-1}), SCO_2 (56.4 ±0.6 mg g^{-1}) and raw rice husk (52.2 ±1.3 mg g^{-1}) was observed. For the fixed, the same behavior was found. The breakthrough time for the optimal conditions were 109, 240, 155 and 385 min for raw rice husk, rice husk treated with assisted ultrasound, supercritical CO_2 and NaOH respectively.

Key words: Adsorption, Batch, Fixed bed, Rice husk, Methylene blue, Alternative treatments.

LISTA DE FIGURAS

LISTA DE TABELAS

SUMÁRIO

1 INTRODUÇÃO

O despejo inadequado de efluentes contendo corantes em corpos de água é um dos maiores problemas ambientais da atualidade. Em geral, os corantes sintéticos são provenientes de diferentes indústrias como: têxteis, tingimento de couro, processamento de alimentos, plásticos, cosméticos, impressão e fabricação de corantes (Yagub e colaboradores, 2014). A estimativa da quantia de efluentes gerados nestas indústrias é bem complexa. Uma indústria têxtil de médio porte, por exemplo, pode gerar em média 25 mil litros diários de efluentes contendo corantes (Dod e colaboradores, 2015; Kant, 2012).

A redução da penetração da luz, da atividade fotossintética, em conjunto com o caráter mutagênico, carcinogênico e tóxico, está entre os principais danos ambientais e de saúde causados devido ao descarte incorreto dos efluentes coloridos (Gupta e Suhas, 2009). Dentre os possíveis métodos de tratamento (coagulação-floculação, precipitação química, filtração, troca iônica, oxidação avançada) de efluentes coloridos, a adsorção se destaca como o principal, devido ao seu baixo custo de implementação e operação, baixo custo energético, alta eficiência e simplicidade de operação (Dotto e colaboradores, 2015)

Desta forma, as pesquisas em adsorção têm focado no desenvolvimento e aplicação de novos materiais. Estes tendem a substituir o adsorvente mais utilizado, o carvão ativado. Com o alto custo de produção e regeneração do carvão ativado, os adsorventes de baixo custo surgiram no meio cientifico (Gupta e Suhas, 2009; Imran e colaboradores, 2012; Wang e colaboradores, 2016; Dotto e colaboradores, 2016). Aliados ao seu baixo custo, disponibilidade e facilidade de reaproveitamento, diferentes técnicas de modificação de superfície têm sido aplicadas para melhorar a capacidade de adsorção (Dotto e colaboradores, 2015). Os adsorventes de baixo custo são materiais provenientes de rejeitos industriais e agrícolas ou produtos secundários e possuem baixa área superficial. Assim existe a oportunidade para a aplicação de técnicas alternativas como, o ultrassom assistido, extração supercrítica com CO_2, ataques básicos e ácidos para melhorar suas características.

Dentre os diferentes tipos de matérias primas passiveis de uso como adsorvente, a casca de arroz se destaca devido à sua grande disponibilidade. Apenas no Rio Grande do Sul a safra de 2015/2016 atingiu uma produção de 7,3 milhões de toneladas. Isso leva a 1,46 milhões de toneladas de casca de arroz

produzidas (Conab, 2016, Soltani 2014). Em conjunto com a disponibilidade, a presença de grupos orgânicos (celulose, hemicelulose e lignina) é de interesse para a adsorção (Thakur, 2014), embora que, a não funcionalização dos grupos e a baixa área superficial demonstram a necessidade de uma modificação superficial antes de sua aplicação como um adsorvente promissor.

Baseado no exposto acima, este trabalho buscou a aplicação de técnicas alternativas para melhorar o potencial adsorvente da casca de arroz em relação ao corante azul de metileno. Realizaram-se as modificações de superfície da casca de arroz com as técnicas de ultrassom assistido, extração supercrítica com CO_2 e ataque alcalino com hidróxido de sódio. Os materiais modificados foram utilizados para adsorção de azul de metileno em batelada e leito fixo.

2 OBJETIVOS

2.1 OBJETIVO GERAL

Este trabalho teve como objetivo aplicar técnicas de modificação de superfície (ultrassom assistido, extração supercrítica com CO_2 e ataque alcalino com hidróxido de sódio) na casca de arroz *in natura* para melhorar seu potencial de adsorção do corante azul de metileno em operações descontínuas (batelada) e contínuas (leito fixo).

2.2 OBJETIVOS ESPECÍFICOS

- Realizar as modificações da superfície da casca do arroz através das tecnologias de ultrassom assistido, extração supercrítica e ataque alcalino;
- Caracterizar os adsorventes utilizando as seguintes técnicas:
    - Espectroscopia no infravermelho por transformada de Fourier (FTIR);
    - Difração de raios-X (DRX);
    - Microscopia eletrônica de varredura (MEV);
    - Espectroscopia de raios-X por dispersão em energia (EDS);
    - Diâmetro de partícula;
    - Massa específica;
    - Esfericidade.
- Determinar as isotermas de adsorção para a casca de arroz *in natura* e para suas respectivas modificações:
    - Aplicar os modelos de Langmuir e Hill aos dados experimentais;
    - Estimar os parâmetros termodinâmicos de adsorção.
- Determinar a condição ótima para a casca de arroz *in natura* para a operação de adsorção de azul de metileno em leito fixo através de um planejamento fatorial 3^2:
    - Aplicar os adsorventes modificados na melhor condição;
    - Aplicar os modelos dinâmicos para o leito fixo.

3 REVISÃO BIBLIOGRÁFICA

Neste capítulo serão abordados os seguintes aspectos: remoção de corantes de efluentes, fundamentos da adsorção, tipos de adsorventes utilizados, operação de adsorção em batelada e continua e seus respectivos modelos matemáticos.

3.1 REMOÇÃO DE CORANTES DE EFLUENTES

Antigamente, a escolha e utilização dos corantes não eram consideradas em relação ao seu impacto ambiental, inclusive, a maioria dos corantes possuía uma composição desconhecida (Gupta e Suhas, 2009). Atualmente efeitos como à redução da penetração de luz e atividade fotossintética, o potencial mutagênico, carcinogênico e tóxico quando ingeridos, são reconhecidos como problemas ambientais e de saúde, devido à exposição aos corantes sintéticos. Devido a estes fatos, diferentes métodos foram desenvolvidos para a remoção dos corantes. Estes podem ser divididos em três tipos: químicos, biológicos e físicos. Suas respectivas vantagens e desvantagens estão apresentadas na Tabela 1 (Yagub e colaboradores, 2014):

Tabela 1 – Técnicas de remoção de corantes.

Técnicas	Vantagens	Desvantagens
Tratamentos químicos		
Processos oxidativos	Simplicidade de aplicação	Agente precisa de ativação
Reação Fenton	Aplicado conforme a característica química	Geração de lodo
Fotoquímico	Redução dos odores e sem geração de lodo	Formação de produtos indesejáveis
Sódio hipoclorito	Inicia e acelera a clivagem das ligações azo	Formação de aminas aromáticas

Destruição eletroquímica	Sem consumo de agentes químicos e de formação de lodo	Altas vazões causam a à redução na remoção dos corantes
Tratamentos biológicos		
Descolorização por fungos	Alguns fungos são capazes de decompor corantes utilizando enzimas	Já foi demonstrado quer a produção de enzimas é inviável.
Mistura de culturas microbianas	Tempo de descolorização de 24 a 30 horas	Sob condições aeróbias os azo corantes não estão prontos para serem metabolizados
Uso de biomassa de microrganismos vivos e/ou mortos	Afinidade relativa ao tipo de corante e microrganismos	Não é efetivo para todos os tipos de corantes
Sistema de biorremediação anaeróbica têxtil-corante	Permite a descolorização de azo corantes e corantes solúveis em água	A quebra anaeróbica gera metano e sulfito hidrogenado
Tratamentos físicos		
Adsorção por carvão ativado	Boa remoção para uma grande quantia de diferentes corantes	Alto custo
Filtração por membrana	Remoção de todos os tipos de corantes	Produção de lodo concentrado
Irradiação	Oxidação efetiva em escala laboratorial	Requer uma grande quantia de O_2 dissolvido
Coagulação eletrocinética	Economicamente praticável	Alta produção de lodo

Fonte: Yagub e colaboradores, 2014, p. 175.

Dentre os possíveis métodos para a remoção de corantes, a adsorção tem se destacado. Isto porque, a maioria dos outros métodos possuem problemas de produção de lodo, produção de químicos secundários, seletividade no tratamento e outros problemas particulares. Outros fatores que corroboram o uso da adsorção são: a possibilidade de utilizar diversos materiais de baixo custo como adsorventes, possuir um baixo custo de implementação e operação, baixo custo energético, alta eficiência e simplicidade de operação (Dotto e colaboradores, 2015)

3.2 ADSORÇÃO

A adsorção é considerada uma operação unitária na qual ocorre a transferência de massa de uma fase fluida (liquida ou gás) para a superfície e interior de uma fase sólida, representada na Figura 1 (McCabe, 1993).

Figura 1 – Representação esquemática da adsorção.

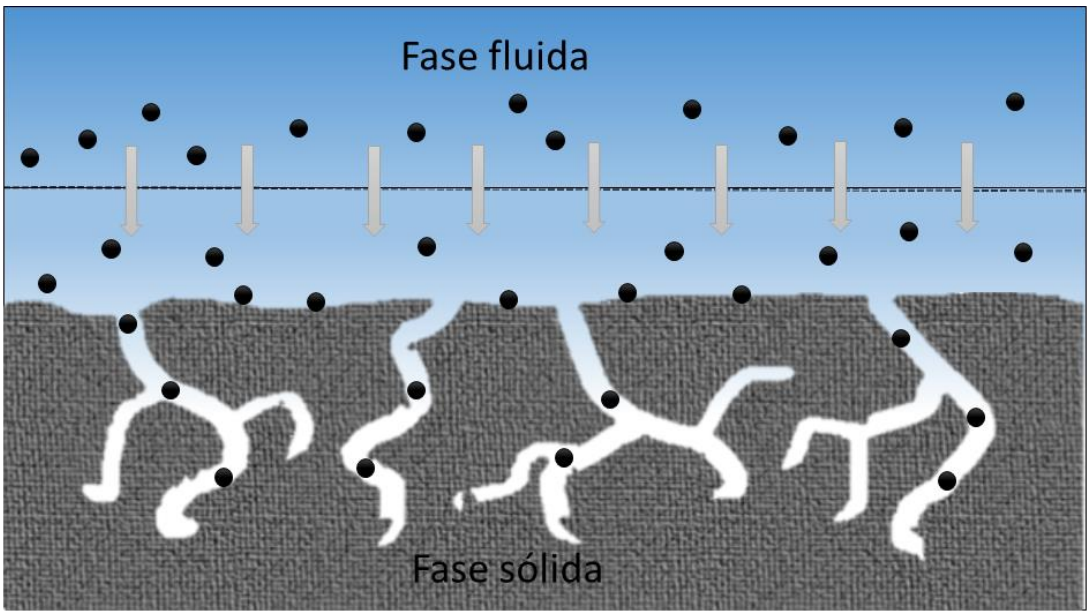

Fonte: o Autor.

A adsorção pode ser distinguida entre dois tipos, a fisiosorção e a quimiosorção, estas dependem apenas das naturezas da força de superfície e do material utilizado. A fisiosorção consiste de forças de repulsão-dispersão (Van der Waals) e forças eletrostáticas de atração (polarização, campo dipolo), em conjunto, não ocorrendo troca de elétrons entre o adsorvente e o adsorbato. A fisiosorção permite a regeneração do adsorvente com mais facilidade. Por outro lado, a

quimiosorção está relacionada com a transferência e/ou divisão de elétrons a fim de formar uma ligação química (Ruthven, 1984).

Usualmente, a pesquisa de adsorção é inicialmente realizada em batelada (Figura 2). Neste caso, o adsorvente fica em contato direto com o fluido durante um determinado tempo, sendo auxiliado por um impulsor ou rotação do vaso, este tem função de manter a transferência de massa uniforme (Brenner, 1994).

Figura 2 – Adsorção em batelada por agitação direta (a) e indireta (b).

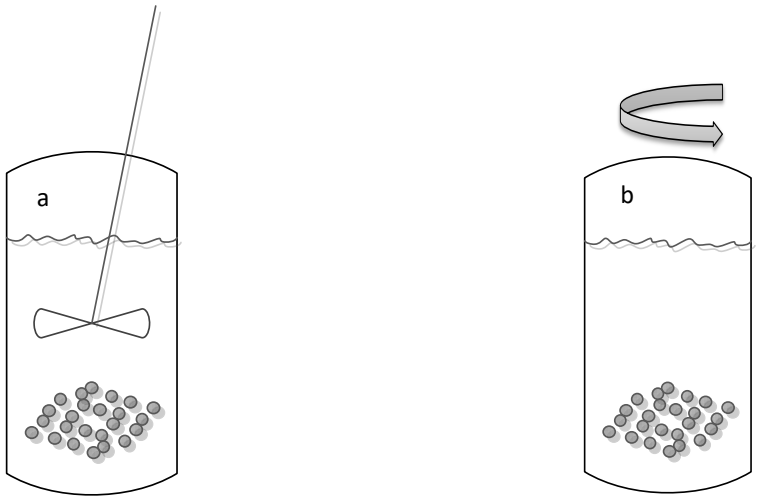

Fonte: o Autor.

Considerando o balanço de massa macroscópico do adsorbato no tanque agitado, que o adsorvente seja inicialmente virgem e que as tomadas de volume para quantificação do adsorbato sejam suficientemente pequenas de modo a não afetar o volume total, é obtida a equação 1:

$$q = \frac{V}{m}\left(C_0 - C\right) \tag{1}$$

onde, q é a capacidade de adsorção (mg g^{-1}), C_0 é a concentração inicial do adsorbato, C é a concentração de adsorbato (mg L^{-1}), V é o volume do fluido (L) e m é a massa de adsorvente (g). Com o uso da equação 1, é possível estimar quanto do adsorbato foi adsorvido no material.

3.3 ISOTERMAS DE ADSORÇÃO

Quando o adsorvente fica em contato com o fluido por tempo suficiente, é alcançado o equilíbrio termodinâmico entre as moléculas de adsorbato nas fases fluída e sólida (Suzuki, 1990). Considerando que este fenômeno ocorra na mesma temperatura, são obtidas às curvas de isotermas de adsorção, estas ajudam no desenvolvimento e aplicação de diferentes materiais como adsorventes.

As isotermas de adsorção são comumente descritas por modelos matemáticos (físicos, empíricos, semi-empíricos), embora os modelos físicos sejam mais fortemente utilizáveis para previsões características da adsorção (Suzuki, 1990). Um dos modelos mais utilizados é o de Langmuir, proposto em 1918, este considera que adsorção acontece em monocamada, e que os sitios do adsorvente são homogêneos e energeticamente iguais, conforme a equação 2 (Langmuir, 1918):

$$q_e = \frac{q_m K_L C_e}{1 + K_L C_e} \tag{2}$$

onde, q_e é a capacidade de adsorção no equilíbrio (mg g^{-1}), C_e é a concentração do adsorbato no equilíbrio (mg L^{-1}), q_m é a capacidade máxima de adsorção (mg g^{-1}) e K_L é a constante de Langmuir (L mg^{-1}). É possível encontrar diversos modelos matemáticos na literatura (exemplos: Freundlich, Redlich-Peterson, Temkin, Dubinin-Radushkevich, entre outros), porém estes modelos sempre possuem a finalidade de predizer as constantes de equilíbrio do sistema.

Paralelamente aos modelos usuais citados acima, Khalfaoui e colaboradores (2003) desenvolveram novos modelos para representar as curvas de isotermas de adsorção. Estes conseguem prever diferentes parâmetros em relação aos modelos clássicos. Estes modelos foram desenvolvidos a partir da física-estatística utilizando a função de partição "*gran canonical ensemble"*. O mais comum é o modelo de Hill, conforme a equação 3:

$$M_a = \frac{nM_M}{1 + \left(\frac{C_{1/2}}{C}\right)^n} = mN_a = \frac{nmN_M}{1 + \left(\frac{C_{1/2}}{C}\right)^n} = N_a = \frac{nN_M}{1 + \left(\frac{C_{1/2}}{C}\right)^n} \tag{3}$$

onde, M_a é a quantia adsorvida (mg g^{-1}), m é massa do adsorbato (mg) ,n é o número de moléculas adsorvidas por sítio, N_M é a densidade do sitio receptor (mg g^{-}

^{1}), N_a é o número de moléculas adsorvidas por sítio e $C_{1/2}$ é a concentração na meia saturação (mg L^{-1}). O número de moléculas adsorvidas por sitio é correlacionado com sua ancoragem, ou seja, a forma na qual a moléculas estão posicionadas em relação à superfície do adsorvente, conforme a equação 4:

$$n' = \frac{1}{n} \tag{4}$$

onde, n' é o número de ancoragem: se n'>1 então a moléculas estarão posicionadas paralelamente em relação a superfície, para n'<1 as molécula se encontram perpendiculares a superfície. Por fim a concentração na meia saturação pode ser relacionada com a energia de adsorção molar, na equação 5:

$$\mathrm{C}_{1/2} = c_s e^{-\Delta E^a / RT} \tag{5}$$

onde, c_s é a solubilidade do adsorbato (mg L^{-1}), ΔE^a é a energia de adsorção molar (kJ mol^{-1}), T é a temperatura (K) e R é a constante universal do gases (8,31x10^{-3} kJ mol^{-1} K^{-1}). Quanto menor for o valor da concentração na meia saturação para uma concentração de solução fixa, maior a quantia adsorvida e maior a energia.

3.4 TERMODINÂMICA DE ADSORÇÃO

Utilizando as isotermas de adsorção, é possível determinar os parâmetros termodinâmicos (ΔS^0, ΔH^0, ΔG^0). Estes servem para indicar a espontaneidade da adsorção, o tipo de adsorção e qual o mecanismo predominante. Os parâmetros podem ser estimados através das equações de Gibbs e de Van't Hoff, 6 e 7, respectivamente (Anastopoulos & Kyzas, 2016):

$$\Delta G^0 = -RT \ln\left(\rho K_e\right) \tag{6}$$

$$\Delta G^0 = \Delta H^0 - T\Delta S^0 \tag{7}$$

onde ΔG^0 é a variação da energia livre de Gibbs padrão (kJ mol^{-1}), ΔH^0 é a variação da entalpia padrão (kJ mol^{-1}), ΔS^0 é a variação da entropia padrão (kJ mol^{-1} K^{-1}), K_e é a constante de equilíbrio (L g^{-1}) e ρ é massa especifica da solução (g L^{-1}).

3.5 ADSORÇÃO EM LEITO FIXO

Outra aplicação da adsorção ligada diretamente com a parte industrial é a utilização do adsorvente em uma coluna, assim denominado leito fixo (Richardson e Harker, 2002). Em geral o fluido a ser tratado entra na parte inferior a uma vazão constante e atravessa o leito, conforme a Figura 3 (Geankoplis, 1993).

Figura 3 – Estrutura do leito fixo de adsorção.

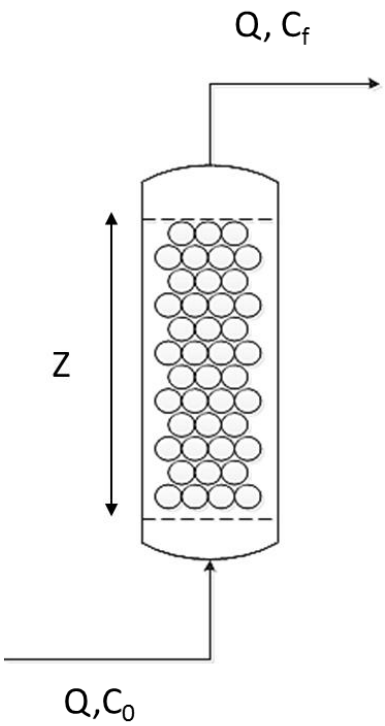

Fonte: o Autor.

Nesta situação a transferência de massa se torna mais complexa que a batelada, já que o processo é transiente e a resistência do leito se torna importante. É considerado que as concentrações do soluto na fase fluida e na fase sólida variam com o tempo e com a posição dentro do leito. Inicialmente é considerado que o adsorvente não possui traços de soluto. Conforme o fluido escoa através do leito, a sua concentração decai rapidamente em relação ao fundo, este comportamento gera um perfil chamado de curva de ruptura, conforme a Figura 4, (Geankoplis, 1993).

Figura 4 – Curva de ruptura para adsorção em leito fixo.

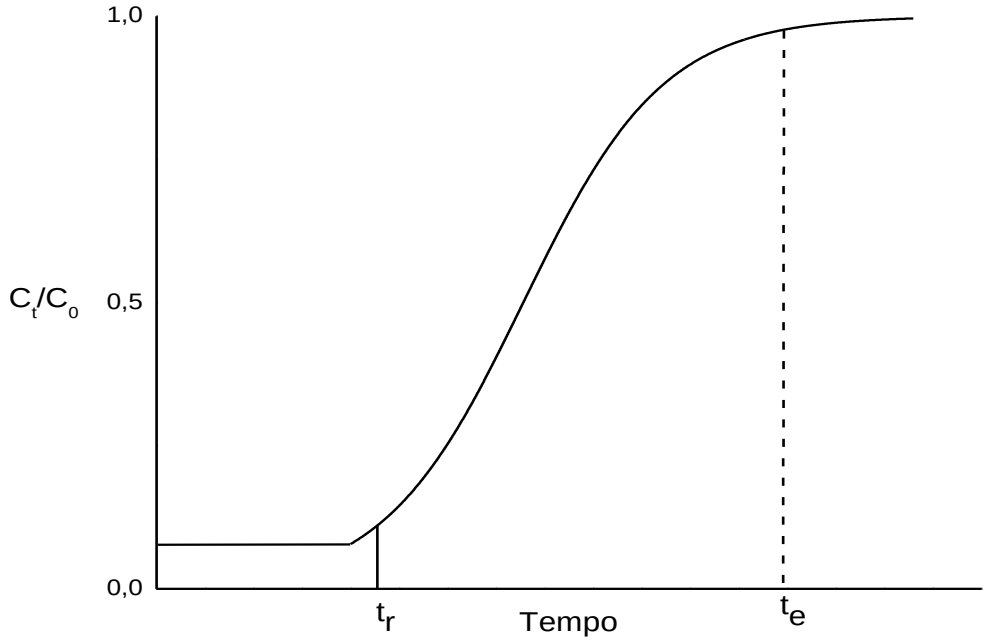

Fonte: o Autor.

Na curva de ruptura é possível estipular dois pontos, o tempo de ruptura (t_r) que corresponde a 0,05 de C_t/C_0 e o de exaustão a 0,95 C_t/C_0 (t_e), estes estão diretamente relacionados com o fenômeno de transferência de massa. Para todos os valores menores que o t_r a concentração de saída da coluna continua inferior a concentração de entrada e a transferência de massa é constante. Após o tempo de ruptura a concentração começa a aumentar rapidamente até que sua concentração inicial seja igual à de saída, isto é, devido à saturação do leito que não consegue mais fazer adsorção (Suzuki, 1990).

Do comportamento da curva de ruptura é possível prever a zona de transferência de massa, que relaciona o menor comprimento possível para o leito obter um t_r, desta forma quanto menor for a zona de transferência de massa melhor será a adsorção, a equação 8 representa a zona de transferência de massa (Suzuki, 1990):

$$Z_m = Z\left(1 - \frac{t_r}{t_e}\right) \tag{8}$$

onde, Z é altura da coluna (cm), t_r é o tempo de ruptura, t_e é o tempo de exaustão e Z_m é a zona de transferência de massa. Outras características sobre a adsorção em coluna podem ser estimadas através da curva de ruptura como, a capacidade de adsorção e o percentual de remoção, de acordo com as equações 9 e 10 (Sugashini e Begum, 2013):

$$q_{eq} = \left(\frac{QC_0}{1000}\right)\frac{A}{m} \tag{9}$$

$$R = \frac{A}{t_{total}}100\% \tag{10}$$

onde Q é a vazão de alimentação (mL min^{-1}), m é a massa de adsorvente (g), C_0 é a concentração inicial do adsorbato (mg L^{-1}), t_{total} é o tempo total de adsorção, A é correspondente a área acima da curva de ruptura, definida pela equação 11:

$$A = \int_0^{t_{total}} \left(1 - {C_t}/{C_0}\right) dt \tag{11}$$

A fim de predizer a curva de ruptura no projeto de leitos fixos, diferentes autores desenvolveram modelos matemáticos que relacionam a capacidade de adsorção e a constante de equilíbrio. Os modelos mais utilizados são os de Thomas, tempo de serviço de altura de leito (TSAL) e Yoon-Nelson, estes estão representados pelas equações 12, 13, 14 respectivamente (Thomas, 1944, Hutchins, 1973 Yoon e Nelson, 1984):

$$\frac{C_o}{C_t} = 1 + \exp\left(\frac{k_{th}q_{eq}m}{Q} - k_{th}C_o t\right) \tag{12}$$

$$\frac{C_o}{C_t} = 1 + \exp\left(\frac{KN_0 h}{u} - KC_o t\right) \tag{13}$$

$$\frac{C_o}{C_t} = 1 + \exp\left(k_{YN}\tau - k_{YN}t\right) \tag{14}$$

onde, k_{th} é a constante de Thomas (mL mg^{-1} min^{-1}), q_{eq} é a capacidade de adsorção no equilíbrio (mg g^{-1}), K é a constante de adsorção (mL mg^{-1} min^{-1}), N_0 é a capacidade de adsorção (mg L^{-1}), h é a altura do leito fixo (cm), u é a velocidade de

escoamento linear (cm min^{-1}), k_{YN} é a constante de Yoon-Nelson (min^{-1}) e τ é o tempo necessário para 50% da curva de ruptura (min^{-1}).

3.6 ADSORVENTES

Apenas quatro tipos de adsorventes genéricos dominam o mercado da adsorção industrial, o carvão ativado, sílica gel, zeólita e alumina ativada. Estes atingiram este patamar devido sua área superficial, poros acessíveis, capacidade de regeneração e reaproveitamento e resistência mecânica (Richardson e Harker, 2002), contudo, seu alto custo de obtenção e regeneração é sua principal desvantagem. Algumas de suas aplicações com líquidos são apresentadas na Tabela 2 (Yang 2003).

Tabela 2 – Principais aplicações dos adsorventes comerciais para líquidos.

Adsorvente	Processo de separação
Sílica, alumina e zeólita	Desidratação, orgânicos oxigenados e halogenados/H_2O
Carvão ativado	Odor e sabor/H_2O
Alumina e zeólita	Compostos sulforosos/Orgânicos
Zeólita	Parafinas, isoparafinas e aromáticos
Carvão ativado	Inorgânicos/H_2O e Orgânicos/H_2O

Fonte: Yang, 2003, p. 5.

O alto custo do carvão ativado e a dificuldade de implementação em larga escala fez com que os adsorventes de baixo custo tenham sido introduzidos na pesquisa (Imran e colaboradores, 2012). Os adsorventes de baixo custo são derivados de fibras naturais, rejeitos agroindustriais e rejeitos sólidos de indústrias (Yagub e colaboradores, 2014). A Tabela 3 apresenta trabalhos da literatura que utilizam adsorventes de baixo custo.

Tabela 3 – Aplicação de adsorventes de baixo custo e corantes utilizados.

Material	Corante	Autor
Caroço de oliva (natural e modificada)	Safranina	Aziz e colaboradores, 2008
Casca de arroz	Laranja Sandocryl	Nawar e Doma, 1989
Casca de coco carbonizada	Azul de metileno	Kannan e Sundaram, 2001
Casca de madeira	Safranina	McKay e colaboradores, 1999
Fibra de palma	Vermelho do congo	Nasser, 1996
Pó de serragem	Azul Astrazon	Asfour e colaboradores, 1985
Semente de mamão	Azul de metileno	Franco e colaboradores, 2012
Quitosana	Azo corantes	Dotto e Pinto, 2011

Fonte:o Autor.

Em conjunto com os materiais apresentados na Tabela 3 existem diversas outras fontes como, resíduos do petróleo, cinzas, bagaço de cana, algas, entre outros (Imran e colaboradores, 2012). Porém uma parte das pesquisas desenvolvidas para adsorventes de baixo custo envolve a fabricação de carvão ativado a partir dos mesmos, de forma física ou química. Isto sugere que as aplicações de outras modificações podem ser estudadas.

3.7 CASCA DE ARROZ E MODIFICAÇÕES ALTERNATIVAS DE SUPERFÍCIE

A casca de arroz é um resíduo agroindustrial proveniente da indústria do beneficiamento de arroz. O uso da casca de arroz como adsorvente é bem conhecido, em especial devido a sua disponibilidade. É possível estimar que 148 milhões de toneladas de casca de arroz são produzidas no mundo, e no Rio Grande do Sul esse valor atinge 1,46 milhões de toneladas (FAO, Soltani e colaboradores, Conab). A casca de arroz é composta principalmente por sílica e grupos orgânicos, celulose, hemicelulose e lignina (Thakur, 2014). A Figura 5 representa sua estrutura

física, porém sua utilidade como adsorvente é limitada devido à baixa área superficial e grupos não disponíveis.

Figura 5 – Arranjo físico da celulose, hemicelulose e lignina.

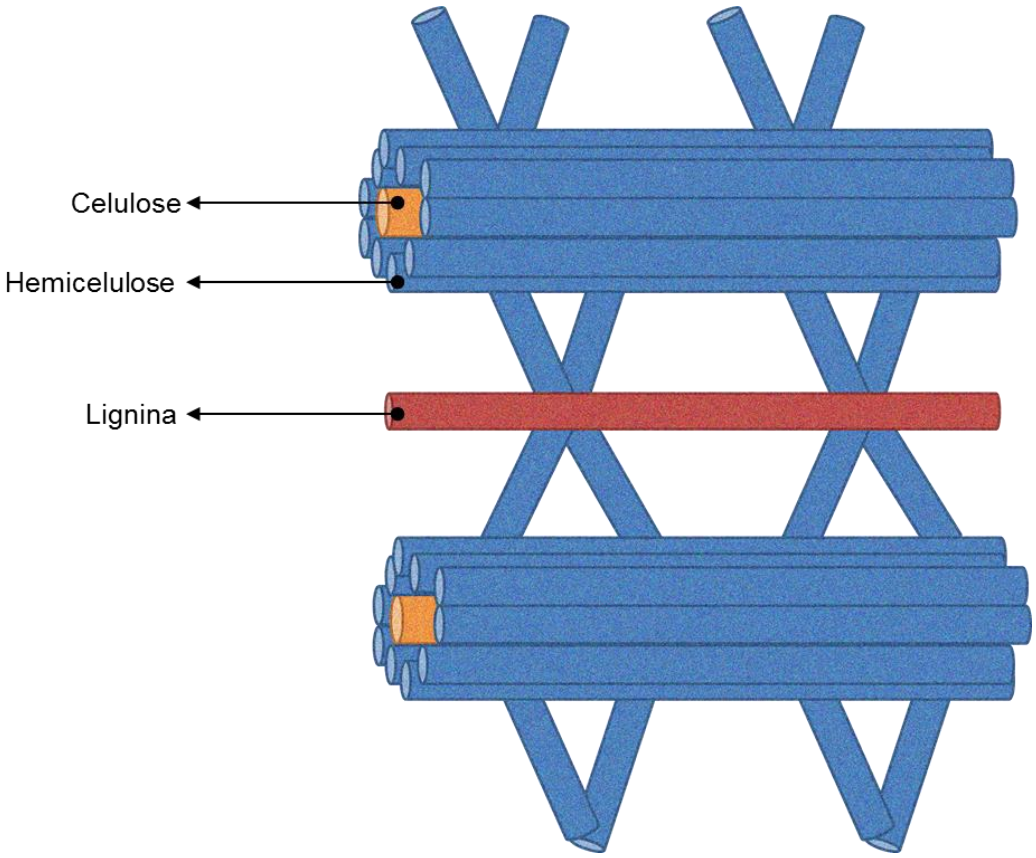

Fonte: o autor.

A utilização de métodos como, extração supercrítica com CO_2, ultrassom assistido e ataques alcalinos (Dotto e colaboradores, 2015, Chakraborty e colaboradores, 2011), tem se demonstrado uma solução alternativa e menos custosa ao processo de carbonização de materiais. Estas técnicas podem romper a casca de arroz devido sua pressão ou cavitação como no supercrítico e ultrassom respectivamente, ou devido à ação da hidrólise pelo uso de bases. Estas modificações podem gerar novos sítios ou espaços vazios levando ao aumento da capacidade de adsorção da casca do arroz.

Dotto e colaboradores (2015) utilizaram a técnica de ultrassom assistido para modificar a estrutura física da quitina. O estudo mostrou que a aplicação do ultrassom causou um aumento de 25 vezes na área superficial da quitina. Além disso, a porosidade foi aumentada e a cristalinidade diminuiu. Estas mudanças na

estrutura da quitina (em relação à quitina in *natura*) levaram a um aumento na capacidade de adsorção do corante azul de metileno. Em outro trabalho, os mesmos autores (Dotto e colaboradores, 2015b) verificaram que o uso de ultrassom e CO_2 em condições supercríticas melhoram a capacidade de adsorção da quitina em relação ao íon cobalto.

Song e colaboradores (2014) realizaram modificações na superfície da casca de arroz utilizando enxofre, organosilanos e hidróxido de sódio, no intuito de melhorar a capacidade de adsorção de mercúrio. Os autores verificaram que a estrutura da casca do arroz foi bastante alterada devido às modificações. Os materiais modificados com enxofre e organosilanos apresentaram melhor desempenho para a adsorção de mercúrio em batelada, com capacidades de adsorção de até 118 mg g^{-1}.

Chakraborty e colaboradores (2011) estudaram a adsorção do corante cristal violeta em batelada utilizando casca de arroz modificada com NaOH. Os autores verificaram que a adsorção foi favorecida pelo aumento do pH e pela diminuição da temperatura. O equilíbrio pode ser descrito pelo modelo de Langmuir. A energia de ativação foi de 50,51 kJ mol^{-1}. Os parâmetros termodinâmicos mostraram que a adsorção foi favorável, espontânea, exotérmica e de natureza química. O mesmo adsorvente foi utilizado por Chowdhury e Saha (2013) para a adsorção do corante verde malaquita em leito fixo. O estudo mostrou que a casca de arroz modificada possui potencial de aplicação industrial para o tratamento de efluentes coloridos.

Os estudos acima mencionados mostram que as modificações de adsorventes de baixo custo (como por exemplo, a casca de arroz) são um viés alternativo para melhorar as características de superfície destes materiais. A melhora nas características, como por exemplo, o aumento da área superficial e porosidade e a diminuição da cristalinidade levam a maiores capacidades de adsorção. Assim, as modificações por ultrassom assistido, extração supercrítica com CO_2 e ataque alcalino com hidróxido de sódio podem ser alternativas para agregar valor e melhorar o potencial adsorvente de um resíduo abundante no Estado do Rio Grande do Sul.

4 RESULTADOS E DISCUSSÃO

Os resultados e discussão deste trabalho estão apresentados na forma de dois artigos, submetidos às revistas *Water Science and Technology* de qualis A2, *Chemical Engineering Communications* de qualis B1 na área de engenharias II.

- ARTIGO 1: ALTERNATIVE TREATMENTS TO IMPROVE THE POTENTIAL OF RICE HUSK AS ADSORBENT FOR METHYLENE BLUE. Dison S. P. Franco, Eduardo H. Tanabe, Daniel A. Bertuol, Guilherme L. Dotto. Submetido à *Water Science and Technology.*

- ARTIGO 2: FIXED BED ADSORPTION OF A CATIONIC DYE USING SURFACE MODIFIED RICE HUSK: STATISTICAL OPTIMIZATION AND DYNAMIC MODELS. Dison S. P. Franco, Daniel A. Bertuol, Eduardo H. Tanabe, Guilherme L. Dotto. Submetido à *Chemical Engineering Communications.*

4.1 ARTIGO 1: ALTERNATIVE TREATMENTS TO IMPROVE THE POTENTIAL OF RICE HUSK AS ADSORBENT FOR METHYLENE BLUE

Dison S. P. Franco[1], Eduardo H. Tanabe[1], Daniel A. Bertuol[1], Guilherme L. Dotto[1]*

[1]Environmental Processes Laboratory (LAPAM), Chemical Engineering Department, Federal University of Santa Maria, 97105-900, Santa Maria, Brazil.

*Corresponding author: e-mail: guilherme_dotto@yahoo.com.br

ABSTRACT

Alternative treatments, such as, NaOH, ultrasound assisted (UA) and supercritical CO_2 (SCO_2), were performed to improve the potential of rice husk as adsorbent to remove methylene blue (MB) from aqueous media. All the treatments improved the surface characteristics of rice husk, exposing its organic fraction and/or providing more adsorption sites. The Langmuir and Hill models were able to explain the MB adsorption for all adsorbents in all studied temperatures. The experimental and modeled parameters demonstrated that the MB adsorption was favored by the temperature increase and, by the use of NaOH-rice husk. The adsorption capacities for the MB solutions (ranging from 10 to 100 mg L^{-1}) were in the following order: NaOH rice-husk (65.0 mg g^{-1})>UA-rice husk (58.7 mg g^{-1})>SCO_2-rice husk (56.4 mg g^{-1})>raw rice husk (52.2 mg g^{-1}). The adsorption was a spontaneous, favorable and endothermic process. In general, this work demonstrated that NaOH, ultrasound assisted (UA) and supercritical CO_2 (SCO_2) treatments are alternatives to improve the potential of rice husk as adsorbent.

Keywords Adsorption, methylene blue, rice husk, surface modification.

INTRODUCTION

Nowadays, the presence of synthetic dyes in effluents has become one of the major concerns to the scientific community. Synthetic dyes are commonly applied in several industries, ranging from leather to plastic and paper (Safa *et al*. 2011; Balci & Ekurt,

2016). The reduction of light penetration and photosynthetic activity, toxicity, mutagenicity and carcinogenicity are examples of the effects caused by the incorrect discharge of the dye containing effluents into the environment (Gupta & Suhas, 2009). In this subject, different techniques have been used for removal and elimination of dyes from effluents, including, adsorption, filtration, ion exchange, advanced oxidation and others. Among these, adsorption stands out due its low cost, low energy requirements, high efficiency, simplicity of implementation and operation (Dotto *et al*. 2015a).

Activated carbon is the most common used adsorbent to remove dyes from effluents. Although it's great performance for adsorption, the manufacturing and regeneration can be costly (Weng *et al*. 2009). Based on this idea, different authors have reported the use of agro industrial wastes as low-cost adsorbents (Ali, 2012; Weber *et al*. 2014; Wang *et al*. 2016; Silva *et al*. 2016; Dotto *et al*. 2016a). Rice husk is a low-cost and available agro industrial waste, achieving 100 million tons per year (Soltani *et al*. 2010), and contains organic compounds as, hemicellulose, cellulose and lignin, which can be potential adsorption sites. Despite of these great advantages, rice husk has low surface area and, several chemical organic structures are non-functionalized or non-accessible for adsorption (Thakur, 2014).

To improve the rice husk performance as adsorbent, the application of chemical or physical surface modifications is an alternative. The surface modifications can increase the surface area and provide new accessible adsorption sites. For this purpose, some modifications were performed on the rice husk surface, including acid or alkaline treatments. The treatment with NaOH, for example, can attack the cellulose chains generating new accessible sites (Soltani *et al*. 2010). Other modifications such as, ultrasound assisted and supercritical CO_2 have been used as viable methods for surface modification of organic materials. It was concluded that these technologies can provide new adsorption sites and an additional porosity (Dotto *et al*. 2015b). In spite of this, the ultrasound and supercritical CO_2 were not yet applied to improve the rice husk characteristics as adsorbent.

In this work, rice husk was modified with NaOH, ultrasound assisted (UA) and supercritical CO_2 (SCO_2) treatments, in order to improve its adsorption potential regarding to the methylene blue (MB) dye. All adsorbents (raw and treated rice husks) were characterized by infrared spectroscopy (FTIR), X-ray diffraction (XRD),

scanning electron microscopy (SEM) and energy dispersive X-ray spectroscopy (EDS). For all materials, experimental equilibrium curves were constructed at different temperatures (from 298 to 328 K). Langmuir and Hill models were used to interpret the equilibrium curves. Also, thermodynamic parameters, such as standard Gibbs free energy change (ΔG^0), standard enthalpy change (ΔH^0) and standard entropy change (ΔS^0) were estimated.

MATERIALS AND METHODS

Obtainment and treatments of rice husk

Raw rice husk was obtained from a local processing industry (Santa Maria RS, Brazil). First, rice husk was washed several times with distilled water, for cleaning and removing any undesirable particles. After, it was dried at 313 K for 24 h and stored for further use. Rice husk was used without milling, with particle size of 5 mm.

Sodium hydroxide treatment: a sodium hydroxide solution (700 mL and 2.5 mol L^{-1}) was poured into a beaker with 20 g of raw rice husk. The suspension was agitated during 2 h and the rice husk was removed. The NaOH treated rice husk was washed with distilled water until achieves neutral pH, and oven dried during 24 h at 313 K. This adsorbent was named NaOH-rice husk.

Ultrasound assisted treatment: for the ultrasound assisted treatment, 20 g of raw rice husk were mixed with 700 mL of distilled water. Then the mixture was treated by an ultrasonic processor (UP400S, Hielscher, Germany) of 400 W equipped with a titanium sonotrode during 2 h. The treatment was performed with cycle of 1 and amplitude of 90% at 313 K. The ultrasound treated rice husk (UA-rice husk) was dried at 313 K during 24 h and stored for further experiments.

Supercritical CO_2 treatment: initially, 20 g of rice husk were put in a sealed jacketed stainless steel 304 reactor at 313 K (the temperature was controlled by a thermostat bath). The CO_2 (White Martins, 99.5%) was pumped and pressurized by a high pressure syringe pump (500D, Teledyne Isco, USA). When CO_2 reached 20 MPa, it was fed into the reactor; then rice husk was exposed to the treatment during 2 h.

Finally the reactor was depressurized and the supercritical treated rice husk (SCO_2-rice husk) was collected and stored.

All the above mentioned treatments and its conditions were determined by preliminary tests and literature (Soltani *et al*. 2010; Dotto *et al.* 2015a,b). The treatments were performed in replicate (n=3).

Characterization techniques

Raw rice husk and the respective modifications (NaOH-rice husk, UA-rice husk and SCO_2-rice husk) were characterized by infrared spectroscopy (FT-IR), X-ray diffraction (XRD), scanning electron microscopy (SEM) and energy dispersive X-ray spectroscopy (EDS). Fourier transform infrared spectroscopy (FT-IR) (Shimadzu, Prestige 21, Japan) was carried out in the range of 500-3500 cm^{-1} to identify the functional groups and the changes caused by the treatments (Silverstein *et al*. 2007). X-ray diffraction (Rigaku, Miniflex 300, Japan) was performed to verify the possible alterations in the amorphous/crystalline structure of the samples (Waseda *et al*. 2011). Scanning electron microscopy (SEM) and energy dispersive X-ray spectroscopy (EDS) were performed (Tescan, Vega3 SB, Czech Republic) to visualize the surface and composition of the samples (Goldstein *et al*. 2003).

Adsorption assays

Methylene blue (MB) (color index 52015, molar weight of 319.8 g mol^{-1}, λ_{max}= 664 nm) was purchased from Vetec, Brazil. All other reagents utilized were of analytical grade, purchased from Sigma-Aldrich. To ensure the experimental accuracy, reproducibility and reliability of the collect data, the adsorption experiments were performed in triplicate; blanks were run in parallel and all dye solutions were stored in glass flasks, which were cleaned by soaking HNO_3 (1.5 mol L^{-1}) for 24 h.

The equilibrium experiments were carried out in a thermostated agitator (Marconi, Ma 093 Brazil) at 298, 308, 318 and 328 K. 5.0 g L^{-1} of each adsorbent was put in contact with MB solutions (initial concentration ranging from 10 to 100 mg L^{-1} and pH of 11.0 (based on preliminary tests)), which were agitated at 150 rpm until equilibrium. All experimental conditions were determined by previous experiments.

The remaining MB concentration in liquid phase was determined using a spectrophotometer (Shimadzu, UV mini 1240, Japan). The equilibrium adsorption capacity (q_e) was determined by:

$$q_e = \frac{V(C_0 - C_e)}{m} \quad (1)$$

where, C_0 is the initial MB concentration in liquid phase (mg L^{-1}), C_e is the equilibrium MB concentration in liquid phase (mg L^{-1}), m is the amount of adsorbent (g) and V is the volume of solution (L).

Langmuir model

The Langmuir model considers that the adsorption occurs in a monolayer, where the binding sites have equal affinity and energy (Langmuir, 1918):

$$q_e = \frac{q_m K_L C_e}{1 + K_L C_e} \quad (2)$$

where, q_m is the maximum adsorption capacity (mg g^{-1}) and K_L is the Langmuir constant (L mg^{-1}).

Hill model

The Hill model is a physical statistical approach developed by Ben Lamine research group. It take in consideration that a variable number c of molecules per unit volume are adsorbed onto N_M receptor sites located on a unit mass of adsorbent (Khalfaoui *et al*. 2003):

$$N_a = \frac{nN_M}{1 + \left(\frac{C_{1/2}}{c}\right)^n} \quad (3)$$

where, n is the number of adsorbed molecule(s) per site, N_M is the receptor sites density, N_a is the number of adsorbed molecule(s), and $C_{1/2}$ is the concentration at half saturation. The stoichiometric coefficient n is related with the anchorage number n':

$$n' = \frac{1}{n} \quad (4)$$

The *n'* parameter describers how the molecule(s) tends to be positioned in relation to the adsorbent surface. If *n'* > 1, the molecules are in parallel with surface and, if *n'* < 1, the molecules are perpendicular to the surface. For a solid-liquid adsorption system the concentration at half saturation can be related with the molar adsorption energy:

$$C_{1/2} = c_s e^{-\Delta E^a / RT} \quad (5)$$

where, c_S is the solubility of the adsorbate, ΔE^a (kJ mol^{-1}) is molar adsorption energy, *T* is the temperature (K), *R* is the universal gas constant (8.31x10^{-3} kJ mol^{-1} K^{-1}).

Thermodynamic parameters

The thermodynamic parameters (ΔS^0, ΔH^0, ΔG^0) were estimated according to the Gibbs and Van't Hoff equations (Anastopoulos & Kyzas, 2016):

$$\Delta G^0 = -RT \ln(\rho K_e) \quad (6)$$

$$\Delta G^0 = \Delta H^0 - T\Delta S^0 \quad (7)$$

where, ΔG^0 is the standard Gibbs free energy change (kJ mol^{-1}), ΔH^0 is the standard enthalpy change (kJ mol^{-1}), ΔS^0 is the standard entropy change (kJ mol^{-1} K^{-1}), K_e is the equilibrium constant (L g^{-1}), *T* is the temperature (K), *R* is the universal gas constant (8.31x10^{-3} kJ mol^{-1} K^{-1}) and ρ is the solution density (g L^{-1}).

Parameters estimation

The equilibrium and thermodynamic parameters were determined by the fit of the models with the experimental data through nonlinear regression. The estimation was based on the minimization of the least squares function using the Quasi-Newton method. The calculations were performed using the Statistic 9.1 software (Statsoft, USA). The fit quality was evaluated by the coefficient of determination (R^2) and average relative error (*ARE*) (Dotto *et al*. 2013):

$$R^2 = \left(\frac{\sum_i^n \left(q_{i,exp} - \overline{q}_{i,exp}\right)^2 - \sum_i^n \left(q_{i,exp} - q_{i,model}\right)^2}{\sum_i^n \left(q_{i,exp} - \overline{q}_{i,exp}\right)^2} \right) \quad (8)$$

$$ARE = \frac{100}{n}\sum_{i=1}^{n}\left|\frac{q_{i,model} - q_{i,\exp}}{q_{i,\exp}}\right| \quad (9)$$

where, $q_{i,model}$ is each value of q predicted by the fitted model, $q_{i,exp}$ is each value of q measured experimentally, $\bar{q}_{i,\exp}$ is the average of q experimentally measured and n is the number of experimental points.

RESULTS AND DISCUSSION

Characteristics of raw and modified rice husks

The FT-IR spectra of raw rice husk (a), NaOH-rice husk (b), UA-rice husk (c) and SCO_2-rice husk (d) are show in Figure 1.

For all samples, the major intense bands were found at 3450 cm^{-1} (OH stretching vibrations), 2910 cm^{-1} (C-H alkane stretch), 1650 cm^{-1} (C=O), 1429 (C-C, C-O ring), 1065 cm^{-1} (Si-O-Si asymmetric stretch), 450 cm^{-1} (Si-O-Si bend). These groups are common for lignocellulosic materials, which contains cellulose, hemicellulose and lignin (Thakur, 2014). In especial the NaOH-rice husk has demonstrated a lower intensity in the 1650 cm^{-1} region. This indicates minor rearrangements of the C=O groups (Silverstein *et al*. 2007). These groups can be potential sites for dye adsorption. For the other samples, the spectra were similar. This indicates that the applied methods were not sufficient to provoke the formation of new links or cause significant breaks in the existent links, implying that only physical modifications occurred in the rice husk.

The XRD patterns of raw rice husk (a), NaOH-rice husk (b), UA-rice husk (c) and SCO_2-rice husk (d) are show in Figure 2. All the samples exhibit the same diffraction planes. Only the intensity was affected. This behavior indicates that the surface treatment changed the rice husk crystallinity. The likely hypothesis is that silica was dragged by pressure in the ultrasound and supercritical treatments, or transferred to the solution when sodium hydroxide was used. This can result into new active sites for MB adsorption.

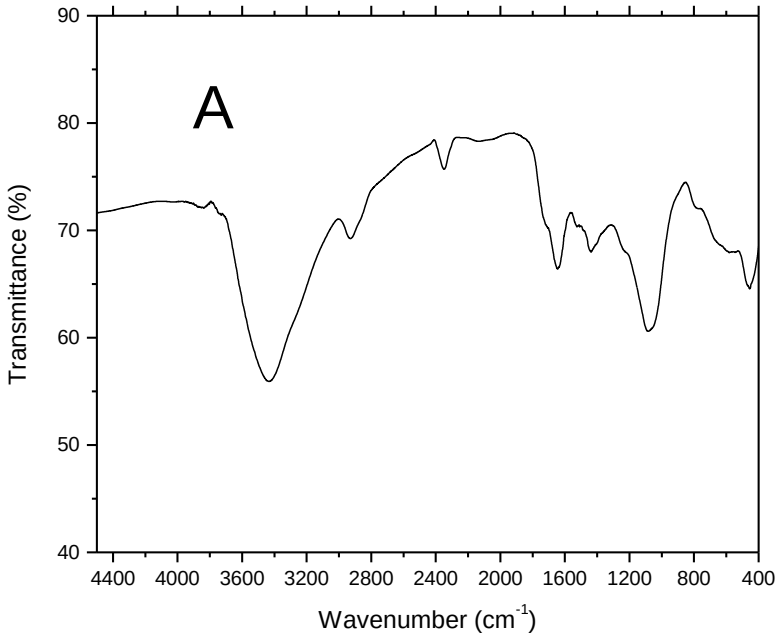
A
Transmittance (%)
90
80
70
60
50
40
4400 4000 3600 3200 2800 2400 2000 1600 1200 800 400
Wavenumber (cm-1)

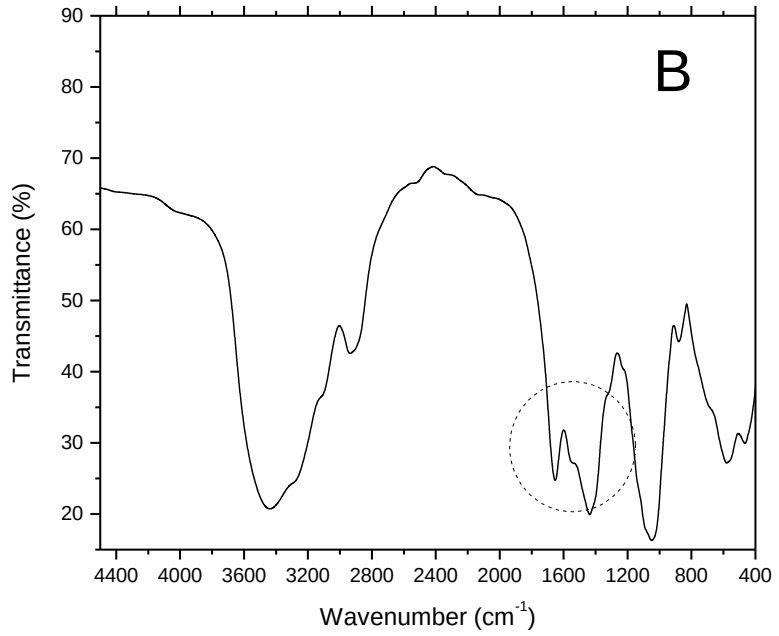
B
Transmittance (%)
90
80
70
60
50
40
30
20
4400 4000 3600 3200 2800 2400 2000 1600 1200 800 400
Wavenumber (cm-1)

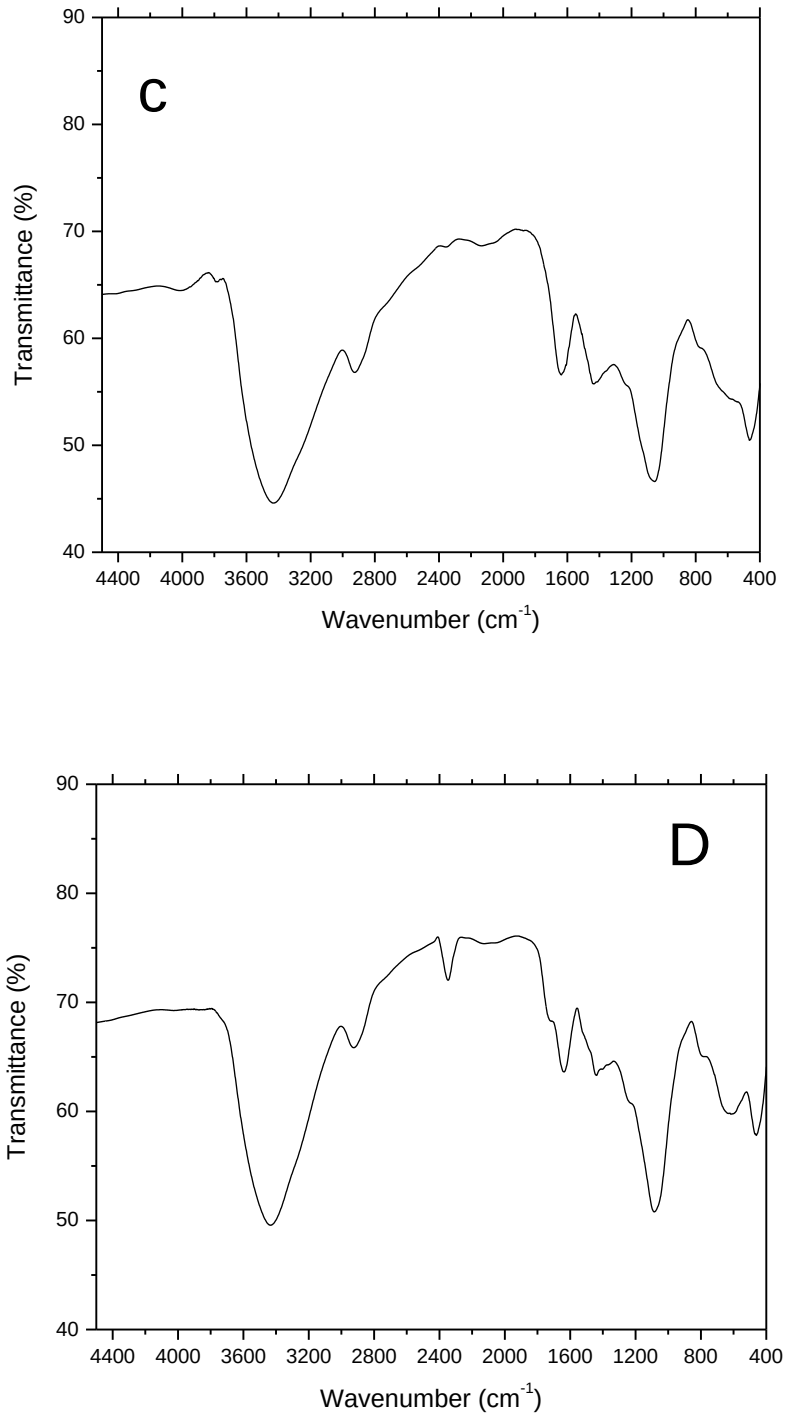

Figure 1 FT-IR spectrum of the raw rice husk (a), NaOH-rice husk (b), UA-rice husk (c) and SCO_2-rice husk (d).

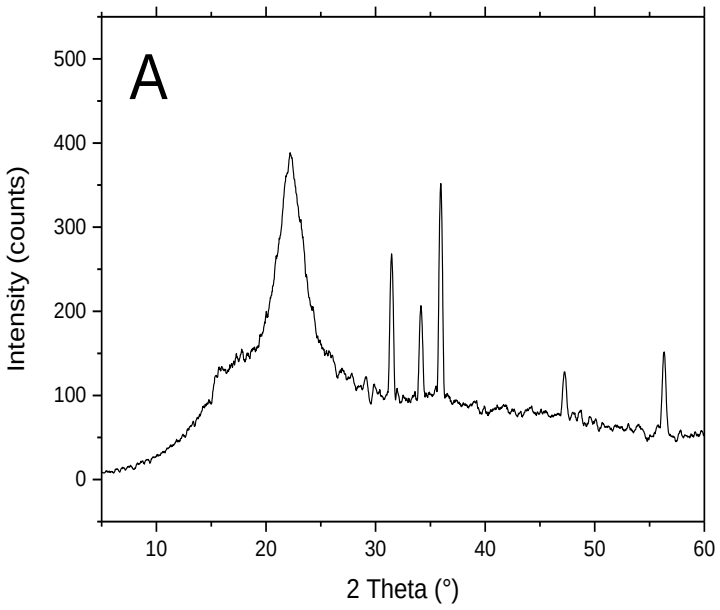
A
Intensity (counts)
2 Theta (°)
0
100
200
300
400
500
10
20
30
40
50
60

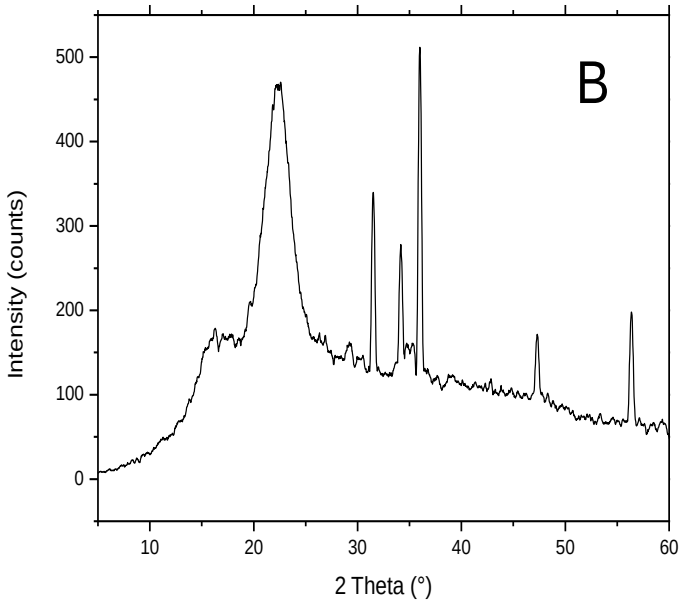
B
Intensity (counts)
2 Theta (°)
0
100
200
300
400
500
10
20
30
40
50
60

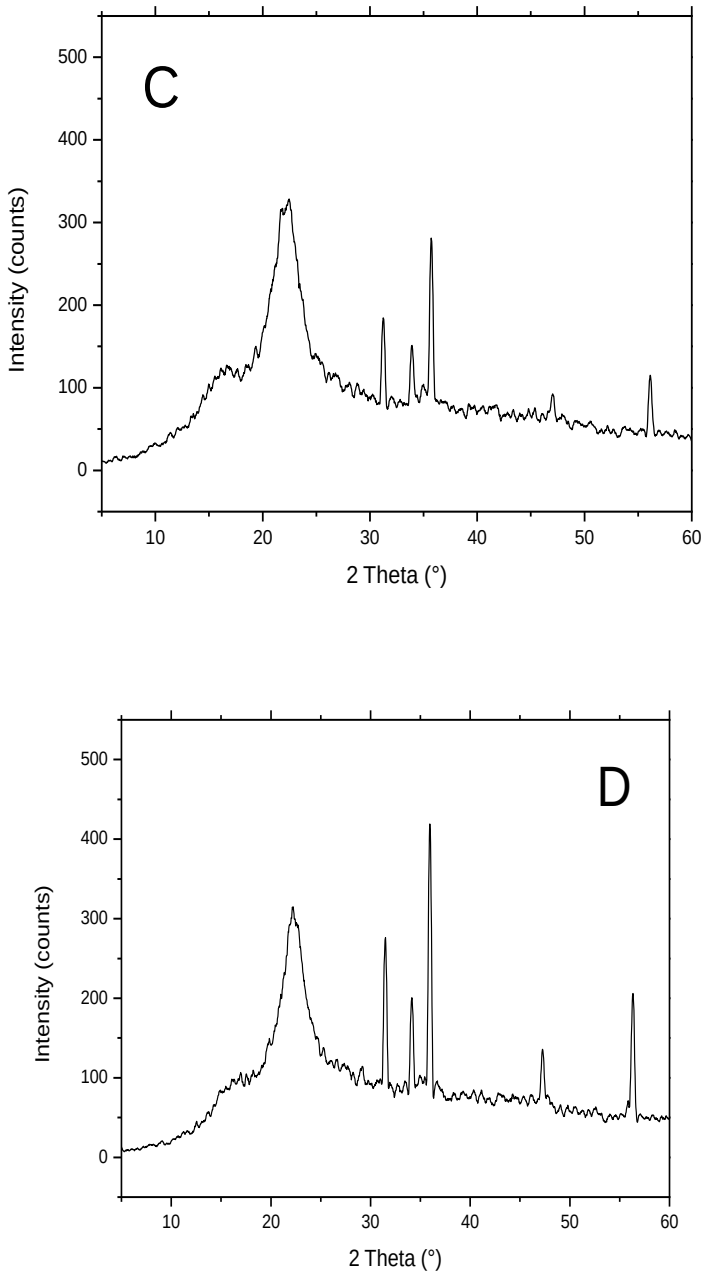

Figure 2 XRD patterns of the raw rice husk (a), NaOH-rice husk (b), UA-rice husk (c) and SCO_2-rice husk (d).

The SEM images of raw rice husk (a), NaOH-rice husk (b), UA-rice husk (c) and SCO_2-rice husk (d) are show in Figure 3. For raw rice husk (a) it can be seen the lemma and the silicate deposit, which is common for this material. In Figure 3 (b) (NaOH-rice husk), it can be verified that strong ruptures on the lemma appeared. As consequence, the endocarp structure (tube cells) was exposed. This can be

favorable for the adsorption process, since allows the diffusion of the MB molecules. For the UA-rice husk (Figure 3 (c)), it can be seen the absence of silicate deposits. This can be favorable for the adsorption process, since expose the organic region to be new interaction sites. The SCO_2-rice husk (Figure 3 (d)) also presents ruptures on the lemma, but, less intense than NaOH-rice husk.

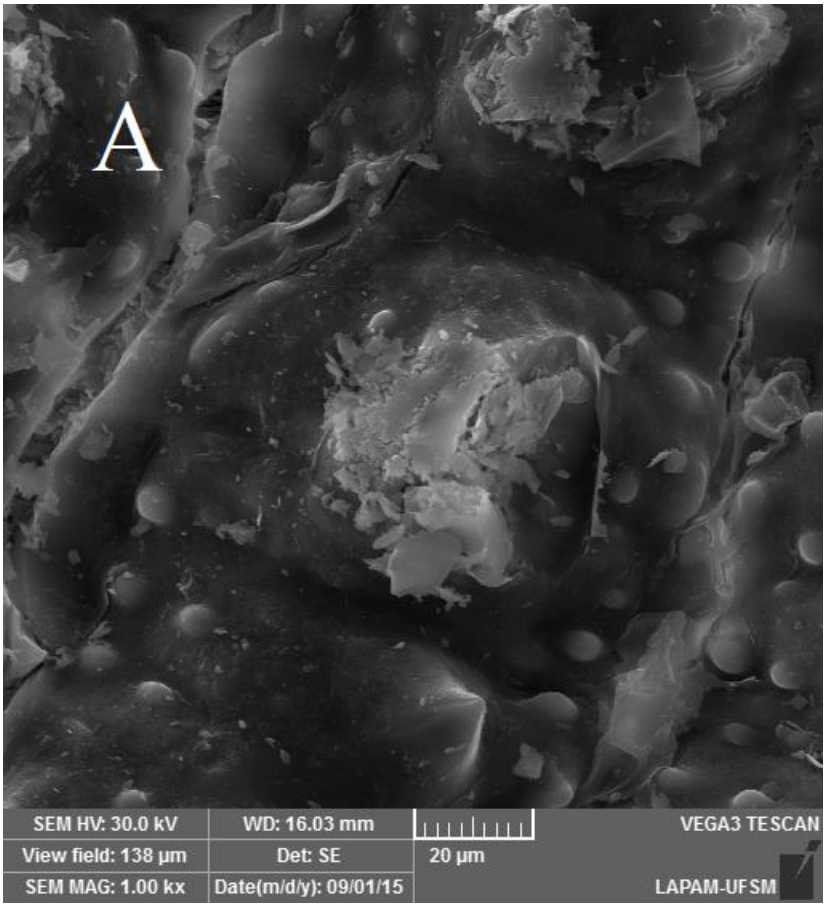

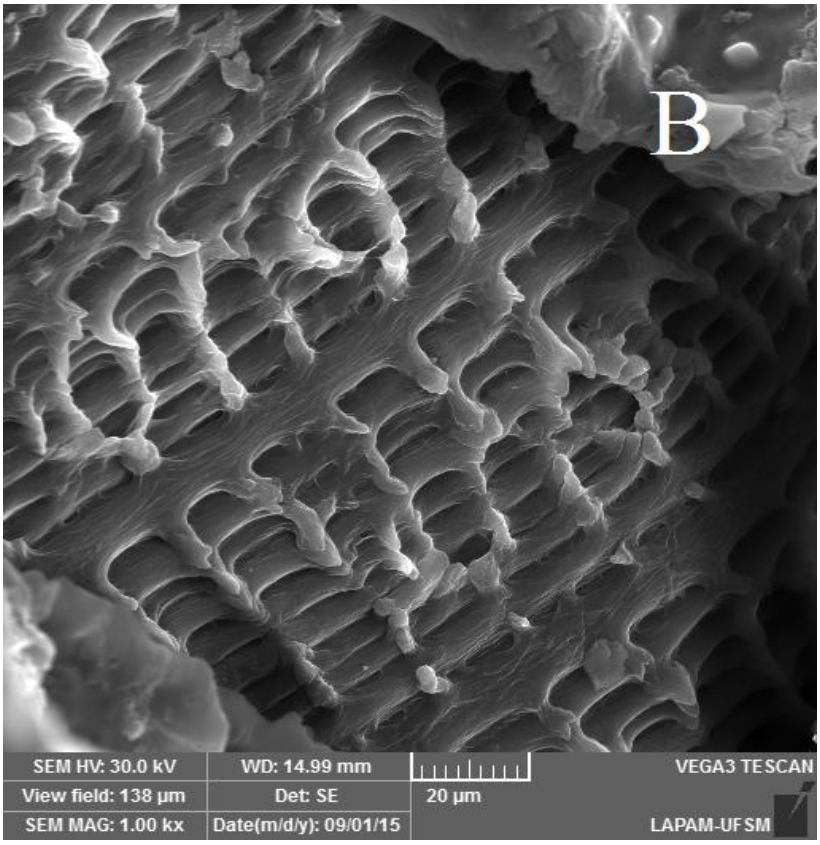
B
SEM HV: 30.0 kV
WD: 14.99 mm
VEGA3 TESCAN
View field: 138 µm
Det: SE
20 µm
SEM MAG: 1.00 kx
Date(m/d/y): 09/01/15
LAPAM-UFSM

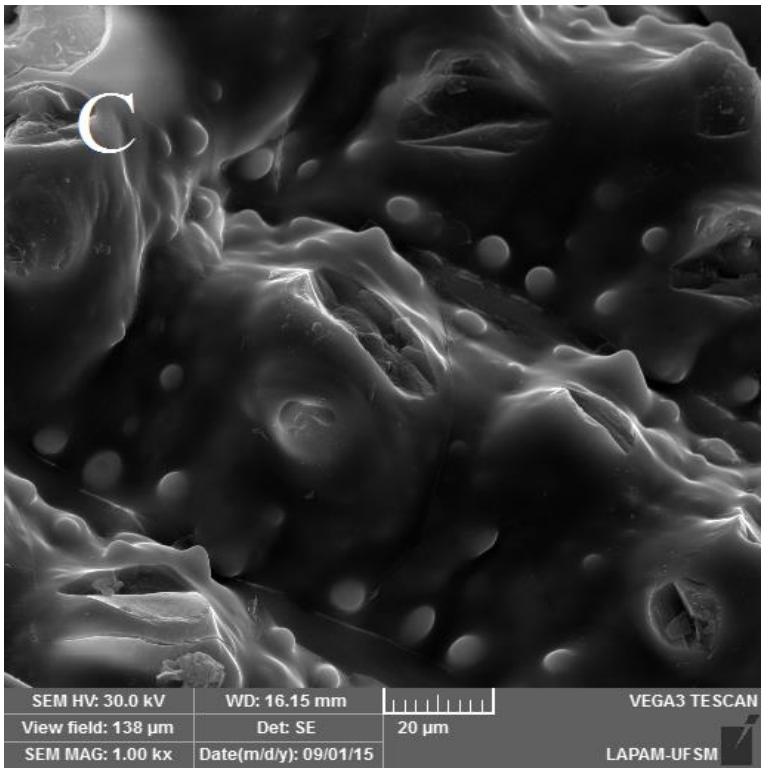
C
SEM HV: 30.0 kV
WD: 16.15 mm
VEGA3 TESCAN
View field: 138 µm
Det: SE
20 µm
SEM MAG: 1.00 kx
Date(m/d/y): 09/01/15
LAPAM-UFSM

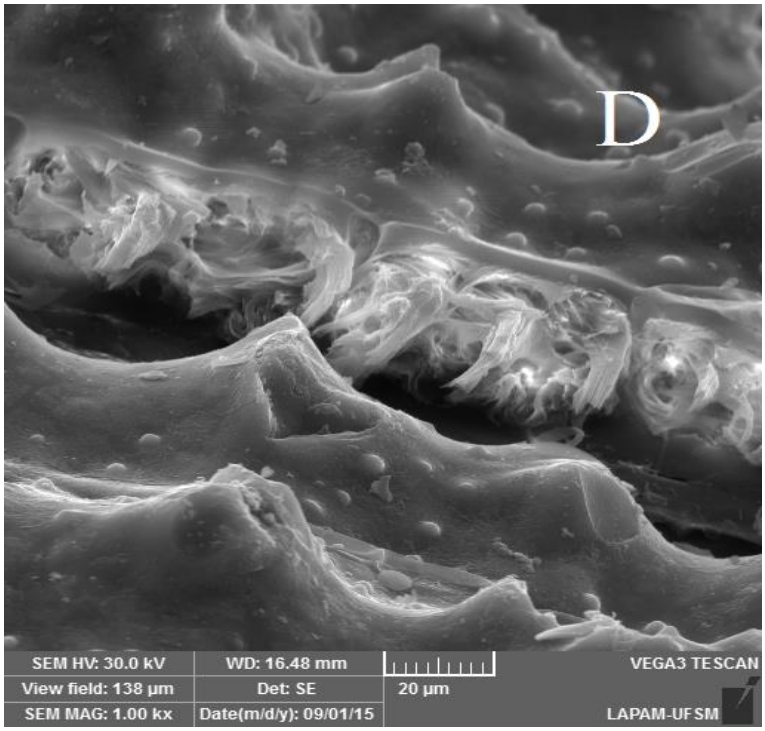

Figure 3 SEM images of the raw rice husk (a), NaOH-rice husk (b), UA-rice husk (c) and SCO_2-rice husk (d).

From the EDS analysis (Figure not shown), it was found that the raw rice husk surface is composed mainly by C, O and Si. For the others samples (NaOH-rice husk, UA-rice husk and SCO_2-rice husk), Si was not detected on the surface. These results corroborates with XRD and SEM analyses. Therefore, it is possible to affirm that the organic fraction of rice husk surface was exposed by the treatments.

Influence of the treatments and temperature on the adsorption isotherms of MB

Figure 4 (Langmuir fit) and Figure 5 (Hill fit) show the equilibrium curves for MB adsorption by raw rice husk (a), NaOH-rice husk (b), UA-rice husk (c) and SCO_2-rice husk (d). Regarding to the temperature effect, it was found that the temperature increase caused an increase in the adsorption capacity. This influence of temperature can be observed for all surface modifications. This suggests that the behavior is related with the overall rice husk composition. Besides, this effect may be attributed to the increase in the number of active sites, or due to the rises of the diffusion rate (Chowdhury *et al*. 2011).

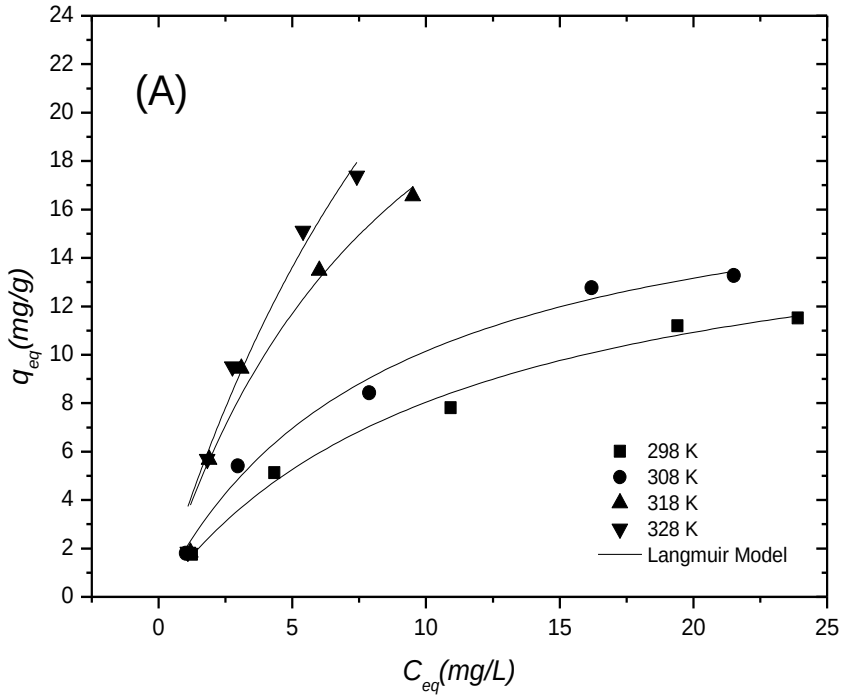
(A)
q_{eq}(mg/g)
C_{eq}(mg/L)
298 K
308 K
318 K
328 K
Langmuir Model

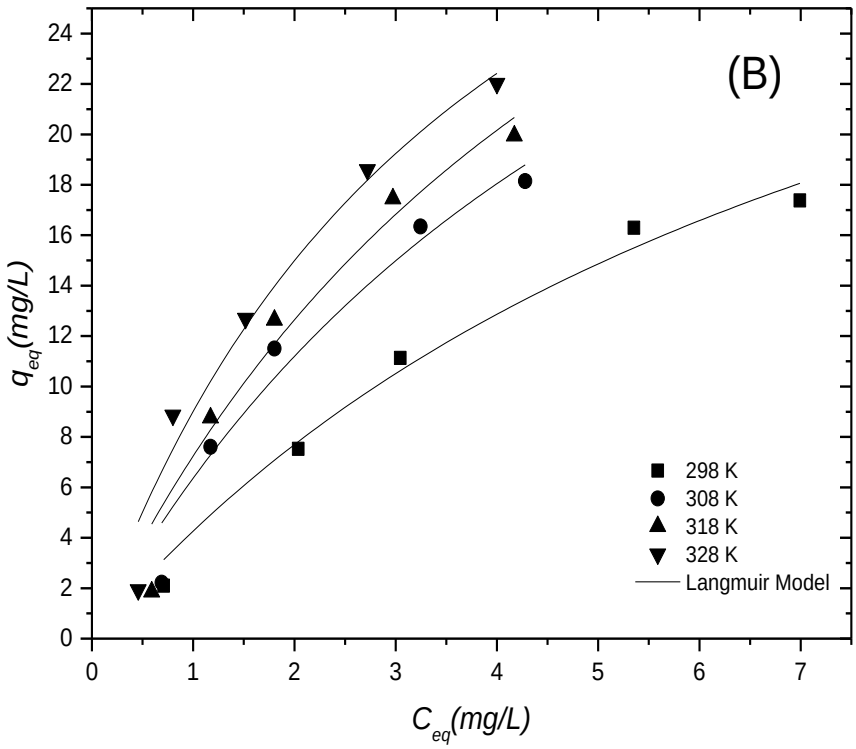
(B)
q_{eq}(mg/L)
C_{eq}(mg/L)
298 K
308 K
318 K
328 K
Langmuir Model

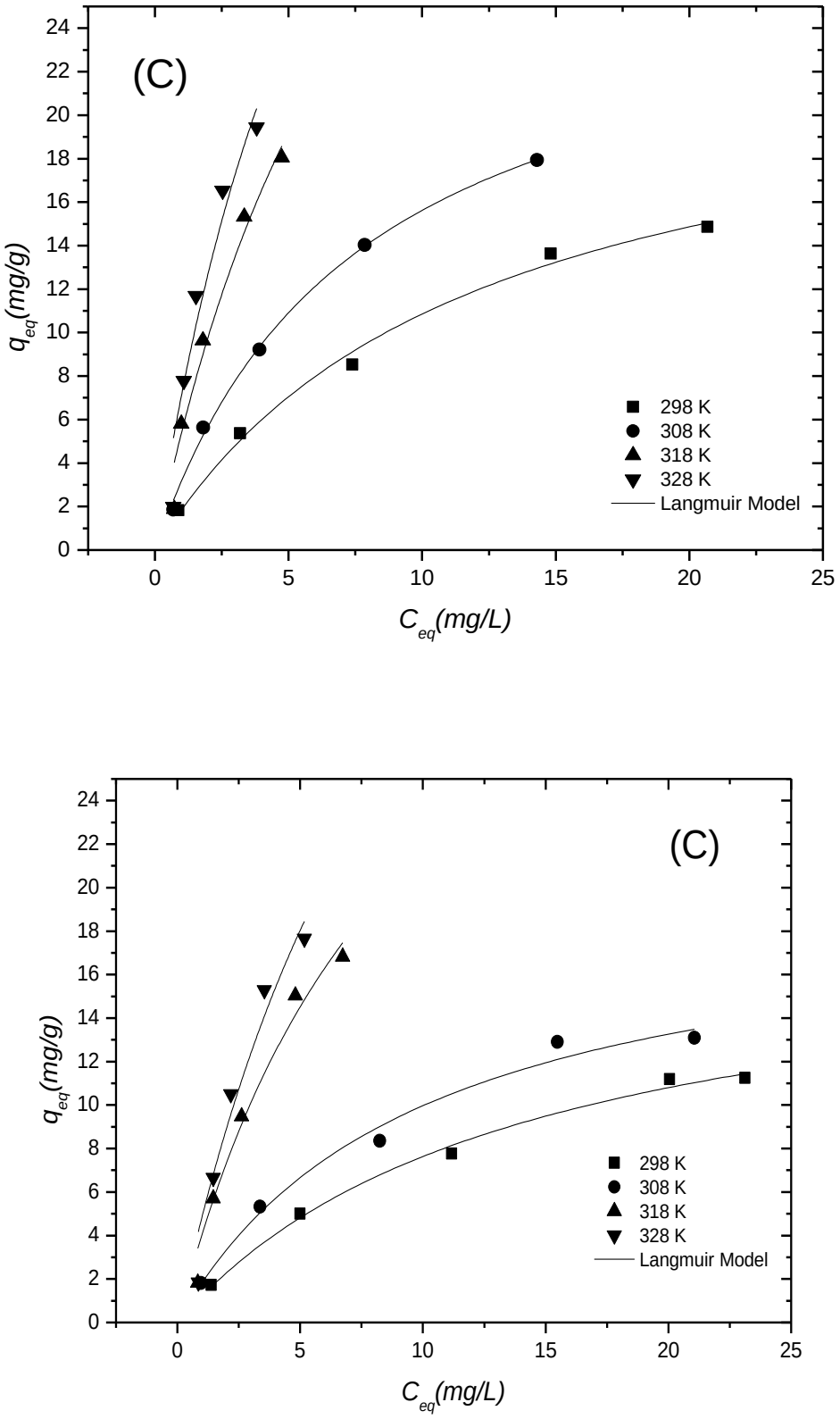

Figure 5 Equilibrium curves for MB adsorption by raw rice husk (a), NaOH-rice husk (b), UA-rice husk (c) and SCO_2-rice husk (d) (Langmuir fitted data).

Regarding to the effect of surface treatments, it was found that, in general, the adsorption capacity followed the order: NaOH rice-husk>UA-rice husk> SCO_2-rice husk> raw rice husk. This shows that all modifications provoked improvements into the rice husk performance as adsorbent. The NaOH-rice husk presented a better adsorption capacity in comparison with the other surface modifications. This can be attributed to the exposure of the endocarp structure (tube cells). This exposure created new adsorption sites and new diffusion paths, which can help the adsorption process (Dotto *et al.* 2015a).

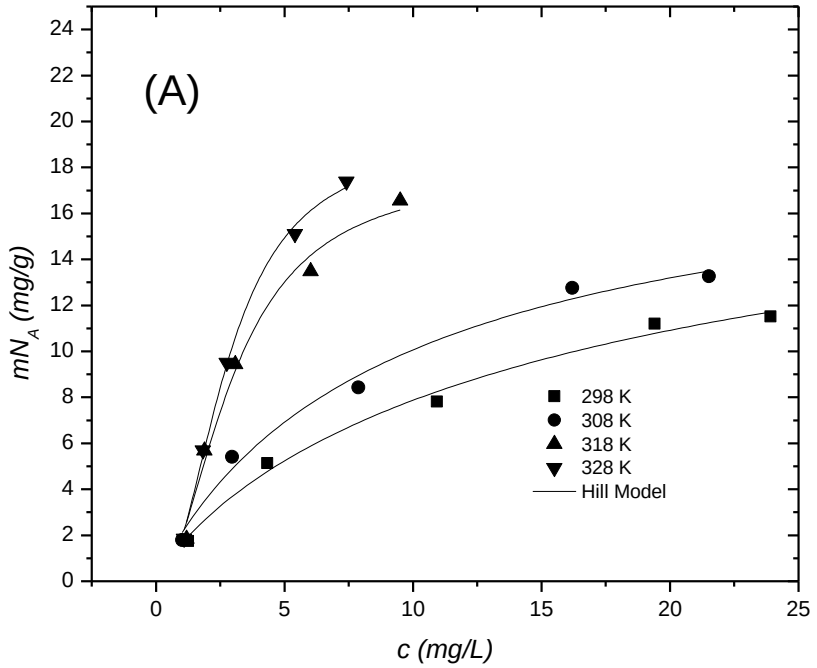

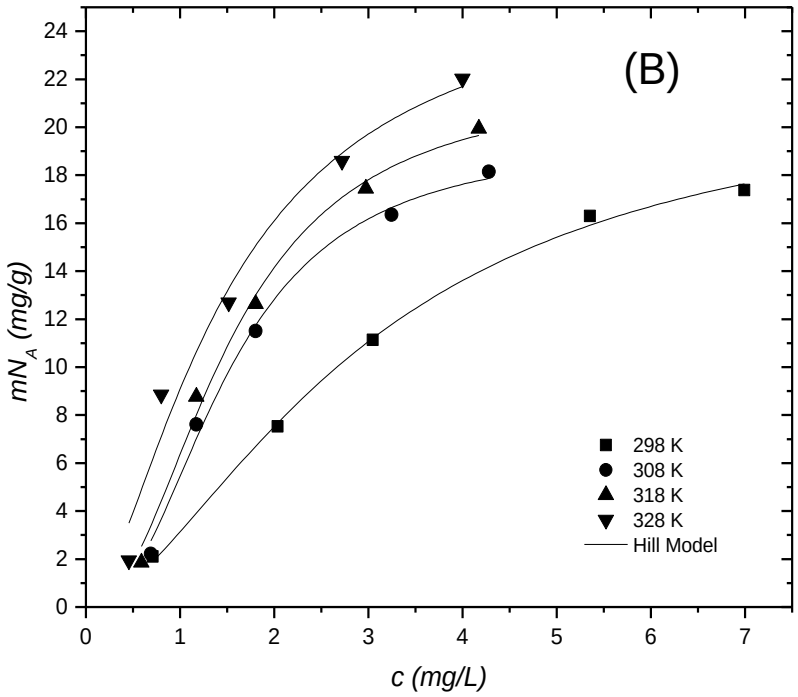

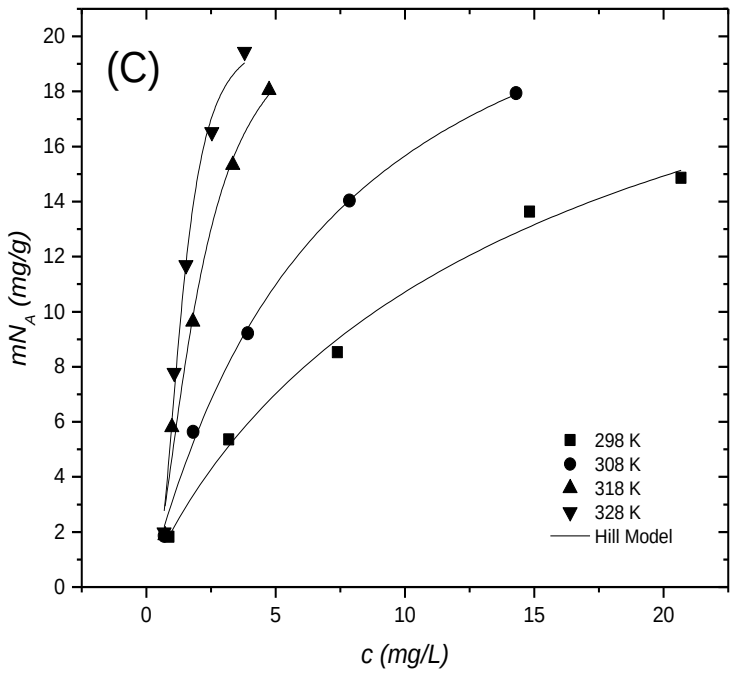

Figure 4 Equilibrium curves for MB adsorption by raw rice husk (a), NaOH-rice husk (b), UA-rice husk (c) and SCO_2-rice husk (d) (Hill fitted data).

Interpretation of Langmuir and Hill models

Table 1 shows the Langmuir parameters for the MB adsorption onto raw rice husk, NaOH-rice husk, UA-rice husk and SCO_2-rice husk. The Langmuir model presented a satisfactory fit with the experimental data (R^2>0.95 and *ARE*<10%). It was found that, for all adsorbents, the temperature increase caused an increase in the q_m values, being the maximum values attained at 328 K. The q_m values were in the following order: NaOH-rice husk, UA-rice husk and SCO_2-rice husk. This behavior indicated that the MB adsorption capacity is favored by the use of NaOH-rice husk at 328 K. In general, the same trend was found by the K_L parameter. This indicated that the affinity adsorbent-adsorbate is higher at 328 K. Also, the higher affinity was found using NaOH-rice husk, confirming that this adsorbent is the more adequate for MB.

Table 1 Langmuir parameters for the adsorption of MB onto raw rice husk, NaOH-rice husk, UA-rice husk and SCO_2-rice husk.

Adsorbent	$T\ (K)$ / Parameters	298	308	318	328
Raw Rice Husk	$q_m\left(mg\,g^{-1}\right)$	17.0±1.5	18.7±1.5	33.5±2.6	52.2±1.3
	$K_L\left(L\,mg^{-1}\right)$	0.089±0.009	0.118±0.004	0.107±0.005	0.069±0.007
	R^2	0.987	0.986	0.959	0.956
NaOH-rice husk	$q_m\left(mg\,g^{-1}\right)$	39.2±2.7	46.5±2.4	49.7±0.6	65.0±0.4
	$K_L\left(L\,mg^{-1}\right)$	0.122±0.007	0.158±0.005	0.17±0.001	0.209±0.003
	R^2	0.979	0.958	0.959	0.954
UA-rice husk	$q_m\left(mg\,g^{-1}\right)$	23.5±2.0	27.4±1.2	52.6±1.4	58.7±2.1
	$K_L\left(L\,mg^{-1}\right)$	0.085±0.001	0.131±0.012	0.114±0.008	0.138±0.005
	R^2	0.979	0.958	0.959	0.954
SCO_2-rice husk	$q_m\left(mg\,g^{-1}\right)$	18.4±1.4	19.7±2.2	42.0±3.8	56.4±0.6
	$K_L\left(L\,mg^{-1}\right)$	0.07±0.001	0.101±0.002	0.105±0.005	0.093±0.005
	R^2	0.979	0.958	0.959	0.954

From the perspective of statistical physical Hill model (R^2>0.97 and *ARE*<10%), it is possible to describe and understand the influence of temperature and surface modifications on the MB adsorption. The Hill parameters are presented in Table 2. According to the literature (Khalfaoui *et al*. 2003; Franco *et al.* 2015, Dotto *et al*. 2016b), the stoichiometric coefficient *n*, describes the adsorption reaction and is a parameter which estimates the numbers of molecules per site during the adsorption process and the adsorbate position on adsorbent surface. This number can be inferior, superior or equal to 1. If this value is inferior to 1, 1/*n* represents the anchorage number of one molecule on several different receptor sites i.e. the molecules adsorb in a parallel position (multi-anchorage) on the adsorbent. If the parameter is superior to 1, i.e. a certain number of molecules are adsorbed on one receptor site. If the number of molecule per site is equal to 1, the molecule interacts by a perpendicular position (mono–anchorage) with the adsorbent surface. In Table 2, it can be noticed that *n* increased with the temperature. The higher *n* values were found for NaOH-rice husk. These results indicate that higher temperatures favored the MB aggregation into the adsorption sites. Also, suggests that the modification with NaOH was efficient, since the surface of NaOH-rice husk is able to interact with more than one molecule per site.

The concentration at half saturation ($C_{1/2}$) decreased with the temperature increase (Table 2), for all used adsorbents. This shows that at higher temperatures, the MB remaining in the solution is low, when the half saturation is attained. One major observation is that, for the NaOH-rice husk, the $C_{1/2}$ value is low, even for the lowest temperatures. This shows that, even at low temperatures, the NaOH-rice husk is a good adsorbent. The last Hill parameter is the adsorbed quantity at saturation (nN_M). In general this parameter presented no clear tendency. However, for NaOH-rice husk, the adsorbed quantity at saturation increased with the temperature, corroborating the above mentioned parameters.

Table 2 Hill parameters for the adsorption of MB onto raw rice husk, NaOH-rice husk, UA-rice husk and SCO_2-rice husk.

Adsorbent	T(K) / Parameters	298	308	318	328
Raw Rice Husk	$C_{1/2}\left(L\,mg^{-1}\right)$	18.3±1.6	9.7±1.8	3.0±0.1	2.8±0.2
	$nN_m\left(mg\,g^{-1}\right)$	21.0±1.4	19.8±6.6	17.9±2.0	19.2±1.2
	n	0.85±0.25	0.94±0.27	1.9±0.44	2.15±0.26
	R^2	0.983	0.983	0.978	0.994
NaOH-rice husk	$C_{1/2}\left(L\,mg^{-1}\right)$	2.9±0.3	1.5±0.1	1.5±0.1	1.4±0.6
	$nN_m\left(mg\,g^{-1}\right)$	19.4±1.7	20.4±1.3	21.8±1.8	26.2±1.3
	n	1.64±0.16	2.31±0.37	2.16±0.39	2.58±0.59
	R^2	0.996	0.989	0.987	0.976
UA-rice husk	$C_{1/2}\left(L\,mg^{-1}\right)$	16.5±1.2	6.8±1.9	1.9±0.5	1.3±0.1
	$nN_m\left(mg\,g^{-1}\right)$	27.5±1.3	26.2±1.3	21.5±2.1	20.1±1.4
	n	0.89±0.21	1.04±0.11	1.82±0.50	2.72±0.52
	R^2	0.989	0.996	0.973	0.983
SCO_2-rice husk	$C_{1/2}\left(L\,mg^{-1}\right)$	20.6±0.2	11.2±0.9	2.6±0.4	1.9±0.1
	$nN_m\left(mg\,g^{-1}\right)$	21.8±1.9	20.8±1.3	20.2±1.1	19.3±1.0
	n	0.89±0.20	0.94±0.33	1.76±0.28	2.37±0.25
	R^2	0.990	0.972	0.991	0.995

Thermodynamic evaluation

The standard Gibbs free energy (ΔG^0), enthalpy (ΔH^0) and entropy (ΔS^0) changes are show in Table 3. For all adsorbents, the ΔG^0 values were negative, confirming that the adsorption was a spontaneous and favorable operation. Also, the temperature increase provided more negative ΔG^0 values, indicating that the adsorption was most favorable at higher temperatures. More negative ΔG^0 values were found for NaOH-rice husk, showing that, the use of this adsorbent, become the operation most favorable. The ΔH^0 values were positive, indicating that the adsorption was endothermic in nature. The magnitude of ΔH^0 is typical of

physisorption (Khalfaoui *et al*. 2003; Franco *et al.* 2015). $T\Delta S^0$ contributed more than ΔH^0 to provide negative ΔG^0 values. This shows that the MB adsorption was an entropy-controlled process.

Table 3 Thermodynamic parameters for the MB adsorption onto raw rice husk, NaOH-rice husk, UA-rice husk and SCO_2-rice husk.

Adsorbent	$T(K)$	$\Delta G^0\left(kJ\ mol^{-1}\right)$	R^2	$\Delta S^0\left(kJ\ mol^{-1}\ K^{-1}\right)$	$\Delta H^0\left(kJ\ mol^{-1}\right)$
Raw rice husk	298	-18.14	0.952	0.14±0.01	24.94±1.73
	308	-19.70			
	318	-21.60			
	328	-22.33			
NaOH rice husk	298	-20.97	0.950	0.13±0.01	19.76±1.18
	308	-22.77			
	318	-23.87			
	328	-25.20			
UA-rice husk	298	-18.80	0.990	0.18±0.01	37.52±1.53
	308	-20.95			
	318	-22.98			
	328	-24.51			
SCO_2 – rice husk	298	-17.75	0.986	0.19±0.01	39.93±1.36
	308	-19.45			
	318	-22.16			
	328	-23.33			

CONCLUSION

In this work, techniques for surface modification were applied on the rice husk, in order to improve its adsorption potential regarding to MB dye. FT-IR, XRD, SEM, and EDS analyses showed that the silica was dragged from the rice husk to the solution and the organic fraction was exposed, creating new adsorption sites. The treatment with NaOH provided the most pronounced surface modification. Regarding to the MB adsorption, Langmuir and Hill models were adequate to represent the equilibrium

data. The MB adsorption was favored by the temperature increase. The adsorption capacities were in the following order: NaOH rice-husk (65.0 mg g^{-1})>UA-rice husk (58.7 mg g^{-1})>SCO_2-rice husk (56.4 mg g^{-1})>raw rice husk (52.2 mg g^{-1}). The thermodynamic parameters demonstrated that the MB adsorption was a spontaneous, favorable, endothermic and entropy controlled process. The magnitude of ΔH^0 is in agreement with physisorption. Based on these results, it is possible to affirm that mainly the NaOH treatment is an alternative to improve the potential of rice husk as adsorbent.

ACKNOWLEDGMENTS

The authors would like to thank CAPES (Brazilian Agency for Improvement of Graduate Personnel) and CNPq (National Council of Science and Technological Development) for the financial support.

REFERENCES

Ali, I. 2012. Low cost adsorbents for the removal of organic pollutants from waste water. *Journal of Environmental Management* **113** (1), 170-183.

Anastopoulos, I., & Kyzas, G. Z. 2016. Are the thermodynamic parameters correctly estimated in liquid-phase adsorption phenomena? *Journal of Molecular Liquids* **218** (1), 174-185.

Balci, B. & Erkurt, F. E., 2016. Adsorption of reactive dye from aqueous solution and synthetic dye bath wastewater by Eucalyptus bark/magnetite composite. *Water Science and Technology* In press, DOI: 10.2166/wst.2016.323.

Chowdhury, S., Mishra, R., Saha, P., & Kushwaha, P. 2011. Adsorption thermodynamics, kinetics and isosteric heat of adsorption of malachite green onto chemically modified rice husk. *Desalination* **265** (1-3), 159-168.

Dotto, G. L., Costa, J. A. V. & Pinto, L. A. A. 2013 Kinetic studies on the biosorption of phenol by nanoparticles from *Spirulina* sp. LEB 18. *Journal of Environmental Chemical Engineering* **1** (4), 1137-1143.

Dotto, G. L., Cunha, J. M., Calgaro, C. O., Tanabe, E. H., & Bertuol, D. A. 2015a. Surface modification of chitin using ultrasound-assisted and supercritical CO_2

technologies for cobalt adsorption. *Journal of Hazardous Materials* **295** (1), 29-36.

Dotto, G. L., Meili, L., de Souza Abud, A. K., Tanabe, E. H., Bertuol, D. A., & Foletto, E. L. 2016a. Comparison between Brazilian agro-wastes and activated carbon as adsorbents to remove Ni(II) from aqueous solutions. *Water Science and Technology* **73** (11), 2713-2721.

Dotto, G. L., Santos, J. M. N., Rodrigues, I. L., Rosa, R., Pavan, F. A., & Lima, E. C. 2015b. Adsorption of Methylene Blue by ultrasonic surface modified chitin. *Journal of Colloid and Interface Science* **446** (1), 133-140.

Dotto, G. L., Sellaoui, L., Lima, E. C., & Lamine, A. Ben. 2016b. Physicochemical and thermodynamic investigation of Ni(II) biosorption on various materials using the statistical physics modeling. *Journal of Molecular Liquids* **220** (1) 129-135.

Franco, D. S. P., Piccin, J. S., Lima, E. C., & Dotto, G. L. 2015. Interpretations about methylene blue adsorption by surface modified chitin using the statistical physics treatment. *Adsorption* **21** (8), 557–564.

Goldstein, J., Newbury, D. E., Joy, D. C., Lyman, C. E., Echlin, P., Lifshin, E., & Michael, J. R. 2003. *Scanning Electron Microscopy and X-ray Microanalysis*. Kluwer Academic/ Plenum Publishers, New York, USA.

Gupta, V. K., & Suhas. 2009. Application of low-cost adsorbents for dye removal - A review. *Journal of Environmental Management* **90** (8), 2313-2342.

Khalfaoui, M., Knani, S., Hachicha, M. A., & Lamine, A. Ben. 2003. New theoretical expressions for the five adsorption type isotherms classified by BET based on statistical physics treatment. *Journal of Colloid and Interface Science* **263** (2), 350–356.

Langmuir, I. 1918 The adsorption of gases on plane surfaces of glass, mica and platinum. *Journal of the American Chemical Society* **40** (9), 1361-1403.

Safa, Y., Bhatti, H. N., Bhatti, I. A., & Asgher, M. 2011. Removal of direct Red-31 and direct Orange-26 by low cost rice husk: Influence of immobilisation and pretreatments. *Canadian Journal of Chemical Engineering* **89** (6), 1554–1565.

Silva, C. E., da Silva Gonçalves, A. H., & de Souza Abud, A. K. 2016. Treatment of textile industry effluents using orange waste: a proposal to reduce color and chemical oxygen demand. *Water Science and Technology* In press, DOI: 10.2166/wst.2016.298**.**

Silverstein, R. M., Webster F. X. & Kiemle D. J. 2007 *Spectrometric Identification of Organic Compounds*. John Wiley & Sons, New York, USA.

Soltani, N., Bahrami, A., & González, L. A. 2014. Review on the physicochemical treatments of rice husk for production of advanced materials. *Chemical Engineering Journal* **264** (1) 899-935.

Thakur, V. K. 2015. *Lignocellulosic Polymer Composites: Processing, Characterization and Proprieties*. Wiley and Scrivener Publishing, New York, USA.

Wang, Y., Zhu, L., Jiang, H., Hu, F., & Shen, X. 2016. Application of longan shell as non-conventional low-cost adsorbent for the removal of cationic dye from aqueous solution. *Spectrochimica Acta Part A: Molecular and Biomolecular Spectroscopy* **159** (1), 254-261.

Waseda, Y., Matsubara, E., & Shinoda, K. 2011. *X-Ray Diffraction Crystallography*. Springer, Berlin, Germany.

Weber, C. T., Collazzo, G. C., Mazutti, M. A., Foletto, E. L. & Dotto, G. L. 2014 Removal of hazardous pharmaceutical dyes by adsorption onto papaya seeds. *Water Science and Technology* **70** (1), 102-107.

Weng, C., Lin, Y., & Tzeng, T. 2009. Removal of methylene blue from aqueous solution by adsorption onto pineapple leaf powder. *Journal of Molecular Liquids* **170** (1), 417-424.

4.2 ARTIGO 2 FIXED BED ADSORPTION OF A CATIONIC DYE USING SURFACE MODIFIED RICE HUSK: STATISTICAL OPTIMIZATION AND DYNAMIC MODELS

Running Head: Fixed Bed Adsorption of MB using modified rice husk

DISON S. P. FRANCO[1], DANIEL A. BERTUOL[1], EDUARDO H. TANABE[1], GUILHERME L. DOTTO[1]*

[1]Environmental Processes Laboratory (LAPAM), Chemical Engineering Department, Federal University of Santa Maria–UFSM, 1000 Roraima Avenue, 97105–900, Santa Maria, RS, Brazil.

*Corresponding author: Chemical Engineering Department, Federal University of Santa Maria–UFSM, 1000 Roraima Avenue, 97105–900, Santa Maria, RS, Brazil.

E–mail address: guilherme_dotto@yahoo.com.br

Abstract

In this work, the fixed bed adsorption of Methylene Blue dye (MB) on surface modified rice husk was investigated. Firstly, rice husk was treated by ultrasound assisted, supercritical CO_2 and NaOH. The adsorbents were characterized. Then, the fixed adsorption was optimized by response surface methodology, using raw rice husk as adsorbent. Finally, under the optimal conditions, breakthrough curves were obtained using all adsorbents and, dynamic models were used to interpret the data. The optimal bed performance was: flow rate of 5 mL min^{-1} and initial MB concentration of 10 mg L^{-1}. Under these conditions, the breakthrough time was 109 min, the length of mass transfer zone was 20.1 cm and the maximum capacity of the column was 1.55 mg g^{-1}. All surface modifications were able to improve the rice husk characteristics, in relation to the MB adsorption. Consequently, the bed performance was significantly improved when the surface modified adsorbents were used. The breakthrough times were 109, 240, 155 and 385 min, for raw rice husk, UA–rice husk, SCO_2–rice husk and NaOH–rice husk, respectively. The length of mass transfer zone was 20.1, 7.9, 15.9 and 9.3 cm for raw rice husk, UA–rice husk, SCO_2–rice husk and NaOH–rice husk, respectively. The dynamic models of Bed Depth Service Time (BDST), Thomas and Yoon–Nelson were able to fit the adsorption data and provided physically consistent parameters.

Keywords Adsorption; Dynamic models; Optimization; Supercritical; Ultrasound.

Introduction

It is estimated that the textile industry generates about 25.000 L of dye containing effluents per ton of manufactured product (Kant, 2012; Dod et al., 2015). These colored effluents can cause different effects to the environment, including reduction of sunlight penetration and photosynthetic activity. Furthermore can be toxic, mutagenic and carcinogenic (Gupta and Suhas, 2009). Methylene Blue (MB) is a cationic dye common in textile effluents, which,

at low concentrations (<2 mg L^{-1}) has many uses, but, is toxic at higher concentrations (Ginimuge et al., 2010).

Currently, several methods are used to remove dyes from colored effluents, such as, chemical precipitation, coagulation/flocculation, advanced oxidation, adsorption and others. Among these, adsorption stands out due its low cost, low energy requirements, high efficiency and ease of operation (Dotto et al., 2015a; Dobre et al., 2016). Fixed bed adsorption is suitable for the treatment of large volumes of colored effluents and, is a fundamental step to scale up the adsorption operation. Activated carbon is the most common adsorbent used in fixed bed adsorption, but, its preparation and regeneration are costly. This aspect makes the search for low cost adsorbents, a field of major interest (Guo et al., 2011; Weng et al., 2009; Gupta and Suhas, 2009).

Rice husk, for example, is a low cost and high available material. Only in the last year, it was estimated a production of 740.2 million tons of paddy rice. As consequence, 148 million tons of rice husk were generated (FAO, 2015; Soltani et al., 2014). In spite of its potential adsorbent, due the presence of organic compounds like, hemicellulose, cellulose and lignin, rice husk has low surface area. This feature is not desirable for adsorption process (Thakur, 2014; Soltani et al., 2014). An alternative to overcome this drawback is the application of surface treatments, such as, ultrasound assisted, supercritical CO_2 or NaOH. The literature shows that these treatments were able to improve the characteristics of some adsorbents (Chakraborty et al., 2011; Lin et al., 2013; Dotto et al., 2015a,b). Based on this literature, it is expected that these treatments provokes surface modifications on the rice husk, which are desirable for MB adsorption. It should be highlighted that the modifications of rice husk using these treatments are scarce in the literature. The majority of these modified materials are applied only in batch adsorption. However, the influence of these surface modifications on the bed performance was not yet investigated.

This work aimed to study the fixed bed adsorption of MB onto raw rice husk and surface modified rice husks. Raw rice husk surface was modified using ultrasound assisted, supercritical CO_2 and NaOH treatments. All samples were characterized by scanning electron microscopy (SEM) and Fourier transform infrared microscopy (FT–IR). Response surface methodology (RSM) was used to optimize the fixed bed adsorption as a function of flow rate and

initial MB concentration, using raw rice husk as adsorbent. The breakthrough time, maximum capacity of the column and mass transfer zone were used as responses. In the optimal conditions, fixed adsorption experiments were performed for the raw and surface modified adsorbents. Finally, Bed Depth Service Time (BDST), Thomas and Yoon–Nelson models were fitted to the experimental data.

Material and Methods

Material obtainment and surface treatments

Raw rice husk was obtained from a local milling industry (Santa Maria, RS, Brazil). At first, rice husk was washed several times to remove any dust or contaminants. After, it was dried at 313 K for 24 h. Raw rice husk surface was then modified using ultrasound assisted, supercritical CO_2 and NaOH treatments. For the ultrasound assisted treatment, raw rice husk was mixed with 700 mL of distilled water and treated using a 400 W titanium processor (Ultrasonic processor, UP400S, Hielscher, Germany) with a cycle of 1 and amplitude of 90%. The supercritical CO_2 (White Martins, 99.5%) treatment was performed using a high pressure syringe pump (500D, Teledyne Isco, USA) at 200 bar, in a sealed jacketed stainless steel 304 reactor. In the sodium hydroxide treatment, raw rice husk was mixed with 700 mL sodium hydroxide solution (2.5 mol L^{-1}) under constant stirring. Each treatment was performed during 2 h using 20 g of rice husk. The samples were named: raw rice husk, UA–rice husk, SCO_2–rice husk and NaOH–rice husk. The samples were stored for further characterization and use. These procedures and conditions were based on preliminary tests.

Characterization techniques

Raw rice husk, UA–rice husk, SCO_2–rice husk and NaOH–rice husk were characterized by scanning electron microscopy (SEM) and infrared spectroscopy (FT–IR). Scanning electron microscopy was performed (Tescan, Vega3 SB, Czech Republic) to visualize the adsorbents surface (Goldstein et al., 1992). Fourier transform infrared spectroscopy (Shimadzu, Prestige 21,

Japan) was performed in the range of 500–3500 cm^{-1} to identify possible changes in the samples functional groups (Silverstein et al., 2007).

Fixed bed adsorption experiments

The cationic dye, Methylene Blue (MB) (color index 52015, molar weight of 319.8 g mol^{-1}, λ_{max}=664 nm, pKa=5.6) was purchased from Plury chemical Ltda., Brazil. This dye was selected since is a common contaminant present in textile effluents.

The fixed bed experiments were conducted in a laboratory scale acrylic column (height 25 cm and diameter 2.5 cm), represented in Figure 1. The colunm was filled with 11.00 g of raw rice husk. The MB solution (pH 11, which was adjusted with NaOH) was pumped from the dye reservoir to the column, by a peristaltic pump (AWG 5900 ABS, Provitec, Brazil). At the column top, samples were collected each 2 min until the bed saturation. The experiments were performed under different flow rates (5, 10 and 15 mL min^{-1}) and initial MB concentrations (10, 30 and 50 mg L^{-1}). The MB concentration was determined using a UV–Vis spectrophotometer (Shimadzu, UV mini 1240, Japan). All experiments were performed in replicate (n=3) and blanks were performed.

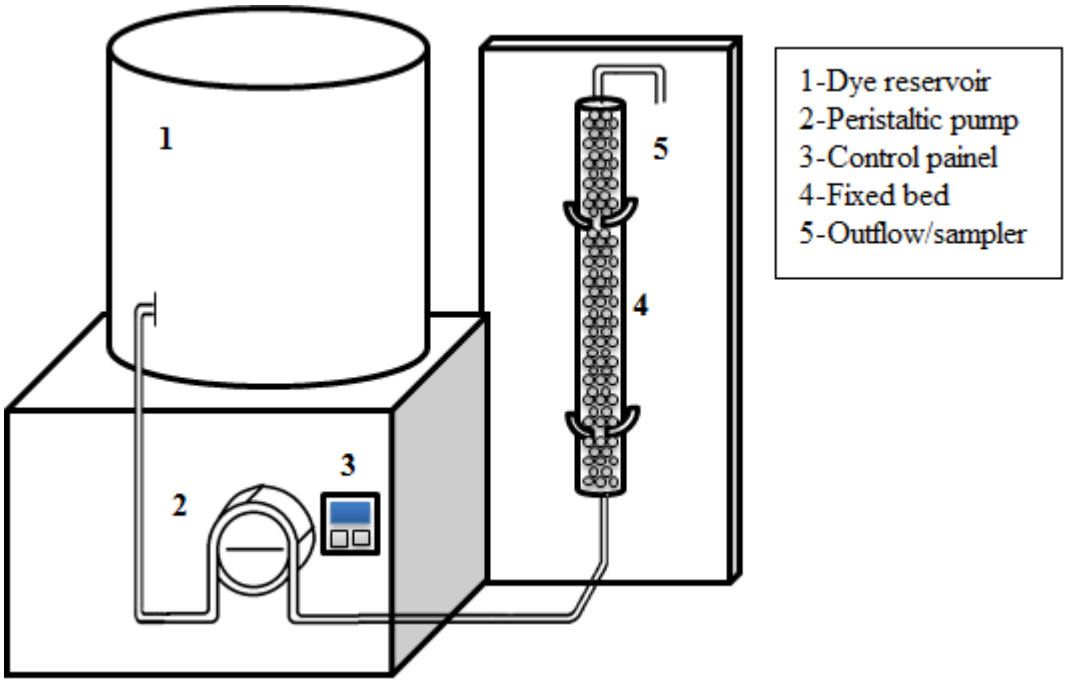

Figure 1: Experimental apparatus for the fixed bed adsorption.

Fixed bed data analysis

The fixed bed adsorption data are generally used to obtain operational parameters. The breakthrough curve is used to obtain the breakthrough time (t_b) and exhaustion time (t_e). These are the times where the outlet flow concentration is equivalent to 5% and 95% of the initial MB concentration, respectively (Suzuki, 1990). Based on the breakthrough and exhaustion times, it is possible to estimate the length of the mass transfer zone (Z_m):

$$Z_m = Z\left(1 - \frac{t_b}{t_e}\right) \quad (1)$$

where, Z is the bed length (cm). This length represents the shortest possible adsorbent bed length necessary to obtain the breakthrough time at t=0 (Suzuki, 1990).

Considering the total adsorption time, it is possible to determine the volume of treated effluent (Dotto et al., 2015a):

$$V_{eff} = Qt_{total} \quad (2)$$

where, Q is the flow rate (mL min^{-1}) and t_{total} is the total operation time (min).

The maximum capacity of the column (q_{eq}) can be estimated by the area above the breakthrough curve:

$$q_{eq} = \frac{\left(\frac{QC_0}{1000}\right)}{m}\int_0^{t_{total}}\left(1 - \left(\frac{C_t}{C_0}\right)\right)dt \quad (3)$$

where, C_0 is the initial MB concentration (mg L^{-1}), C_t is the MB concentration along the time (mg L^{-1}) and m is the adsorbent amount (g).

The MB removal percentage (R) can be estimated as:

$$R = \frac{100}{t_{total}}\int_0^{t_{total}}\left(1 - \left(\frac{C_t}{C_0}\right)\right)dt \quad (4)$$

The numerical values of the area above the breakthrough curve were estimated by Origin (Origin Lab Corp., USA) software using the analysis/calculus/integrate tool.

Statistical optimization

The fixed adsorption of MB onto raw rice husk was optimized by response surface methodology (RSM) (Myers and Montgomery, 2002). The effects of flow rate (Q) (5, 10 and 15 mL min^{-1}) and initial MB concentration (C_0) (10, 30 and 50 mol L^{-1}) were investigated. The breakthrough time (t_b), maximum capacity of the column (q_{eq}) and length of transfer zone (Z_m) were used as responses. A quadratic polynomial model was used to represent the dependent variables as a function of the studied effects. The statistical significance and prediction of the models were determined by Student's and Fischer tests, respectively. The model variance was explained by the coefficient of determination (R^2). All experiments were performed at random and the results were analyzed by Statistic 9.1 software (Statsoft, USA).

Dynamic models

In the optimal conditions for fixed adsorption, which were obtained using raw rice husk, new breakthrough curves were constructed for MB adsorption on UA–rice husk, SCO_2–rice husk and NaOH–rice husk. The Bed Depth Service Time (BDST), Thomas and Yoon–Nelson models were fitted with these experimental data.

The bed depth service time (BDST) model assumes that the adsorption rate is proportional to the residual capacity of the adsorbent and the concentration of the adsorbing species (Hutchins, 1973):

$$\frac{C_0}{C_t} = 1 + \exp\left(\frac{KN_0h}{u} - KC_0t\right) \quad (6)$$

where K is the adsorption constant rate (mL mg^{-1} min^{-1}), N_0 is the adsorption capacity (mg L^{-1}), h is the height of the fixed–bed (cm) and u is the linear flow rate (cm min^{-1}).

The Thomas model is also used to represent and predict the breakthrough curves. This model considers that the adsorption process has a second order reversible kinetics and follows the Langmuir isotherm (Thomas, 1944):

$$\frac{C_0}{C_t} = 1 + \exp\left(\frac{k_{th}q_{eq}m}{Q} - k_{th}C_0t\right) \quad (7)$$

where, k_{th} is the constant of Thomas (mL mg^{-1} min^{-1}) and q_{eq} is the equilibrium adsorption capacity (mg g^{-1}).

The Yoon–Nelson model is also used to represent breakthrough curves (Yoon and Nelson, 1984):

$$\frac{C_0}{C_t} = 1 + \exp\left(k_{YN}\tau - k_{YN}t\right) \quad (8)$$

where, k_{YN} is the constant rate of Yoon–Nelson (min^{-1}) and τ is the time required for 50% of the adsorbate breakthrough (min).

The parameters of the dynamic models were estimated by the fit of the models with the experimental data through nonlinear regression. The models were fitted in its original form. The estimation was based on the minimization of the least squares function using the Quasi–Newton method. The calculations were realized using the Statistic 9.1 software (Statsoft, USA). The fit quality was measured through the coefficient of determination (R^2) and sum of squared errors (SSE) (Dotto et al., 2013).

Results and discussion

Adsorbents characterization

Raw rice husk, UA–rice husk, SCO_2–rice husk and NaOH–rice husk were characterized by SEM and FT–IR. Also, the particle size, specific mass and sphericity were determined (Tanabe et al., 2016). The particle size, specific mass and sphericity presented no significant differences between the samples ($p>0.05$). For all samples, the particle size was 5.7±0.3 mm, the specific mass was 135±5 kg m^{-3} and the sphericity was 0.35±0.02. This indicates that the employed treatments caused no macroscopic changes on the rice husk.

The SEM images of raw rice husk, NaOH–rice husk, UA–rice husk and SCO_2–rice husk are shown in Figure 2. For raw rice husk (a), it can be seen the surface (lemma) and the silica deposits. In the NaOH–rice husk (b) the lemma was torn, exposing the tube cells. In the UA–rice husk (c), the silica deposits on the surface disappeared. The SCO_2–rice husk (d) presented minor exposures of the tube cells. The SEM images indicated that microscopic modifications occurred on the rice husk surface after the treatments. It is expected that these modifications are favorable for MB adsorption, due to the exposure of more

active sites. Similar surface modifications were found by Chakraborty et al. (2011) in the adsorption of Crystal Violet from aqueous solution onto NaOH–modified rice husk and Dotto et al. (2015a) in the adsorption of MB on ultrasonic surface modified chitin.

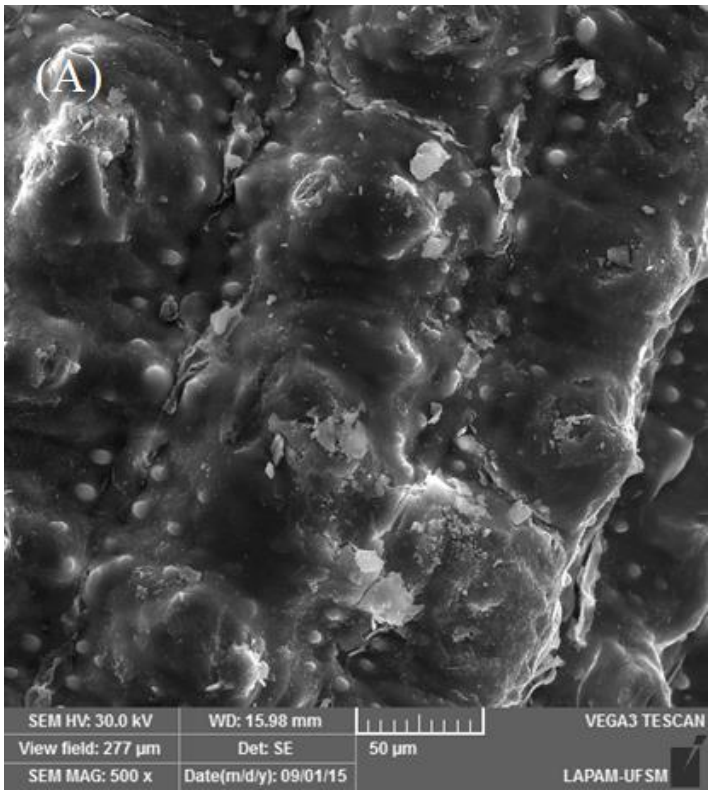

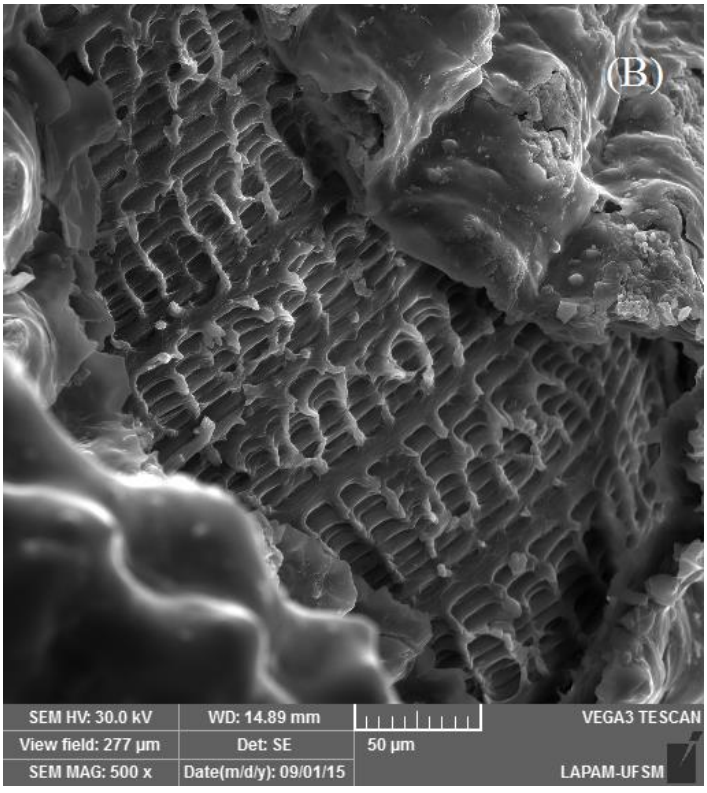

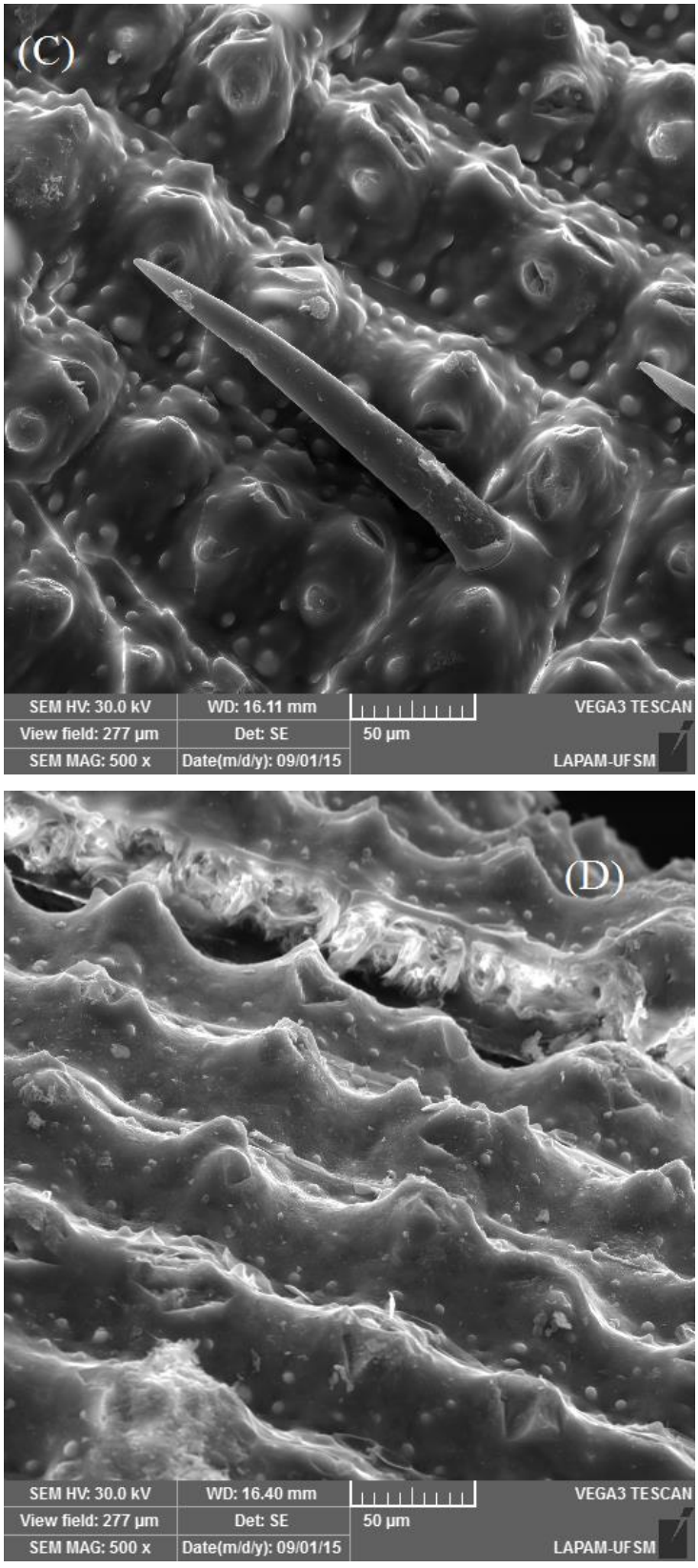

Figure 2: SEM images of (A) raw rice husk, (B) NaOH–rice husk, (C) UA–rice husk and (D) SCO_2–rice husk.

FT–IR showed that no new bands were formed/removed in comparison with the raw rice husk. The main identified groups are presented in Table I.

Table I: FT–IR bands and assignments for raw rice husk.

Bands (cm^{-1})	Assignments
450	Si–O–Si bend
1065	Si–O–SI asymmetric stretch
1429	C–C, C–O ring
1650	C=O
2910	C–H alkane stretch
3450	–OH stretching vibrations

These groups are constituents of cellulose, hemicellulose and lignin and are commonly present in lignocellulosic materials (Thakur, 2014), such as rice husk. FT–IR suggests that the applied treatments affected only the physical characteristics of the rice husk, since the formation or break of new links weren't detected.

Column data interpretation

The column experimental data (breakthrough curves) obtained at different flow rates and initial MB concentrations are presented in Figure 3. All operational conditions and process variables, such as, breakthrough time, exhaustion time, length of mass transfer zone, volume of effluent, maximum capacity of the column and removal percentage are presented in Table II.

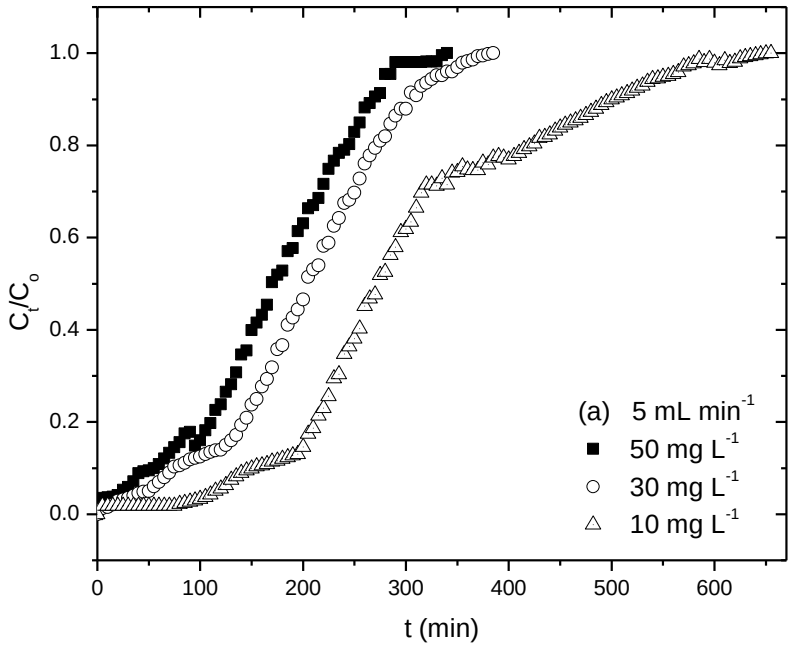
1.0
0.8
0.6
0.4
0.2
0.0
C_t/C_o
0
100
200
300
400
500
600
t (min)
(a) 5 mL min^{-1}
50 mg L^{-1}
30 mg L^{-1}
10 mg L^{-1}

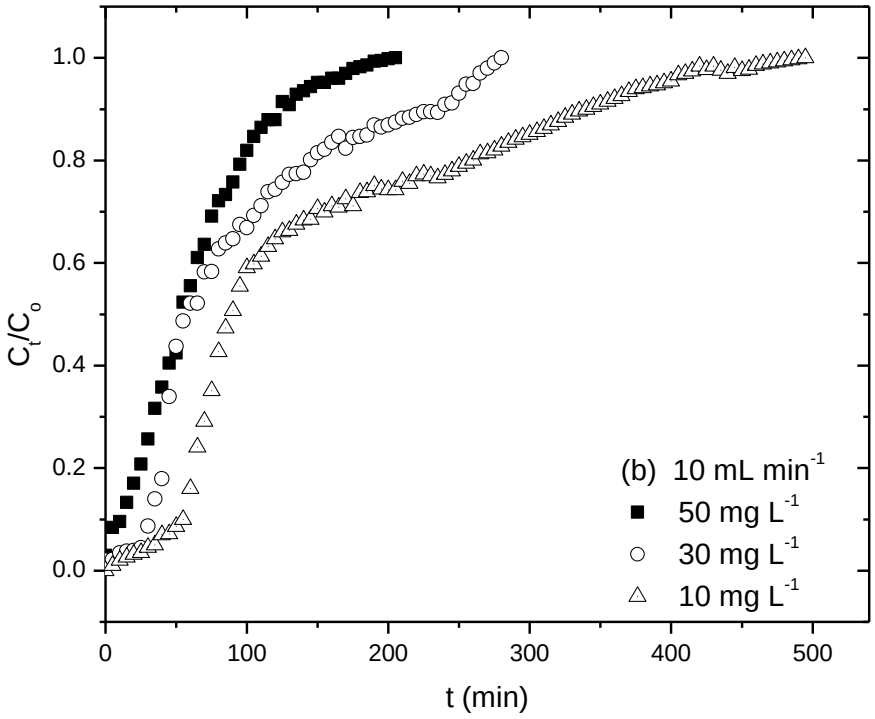
1.0
0.8
0.6
0.4
0.2
0.0
C_t/C_o
0
100
200
300
400
500
t (min)
(b) 10 mL min^{-1}
50 mg L^{-1}
30 mg L^{-1}
10 mg L^{-1}

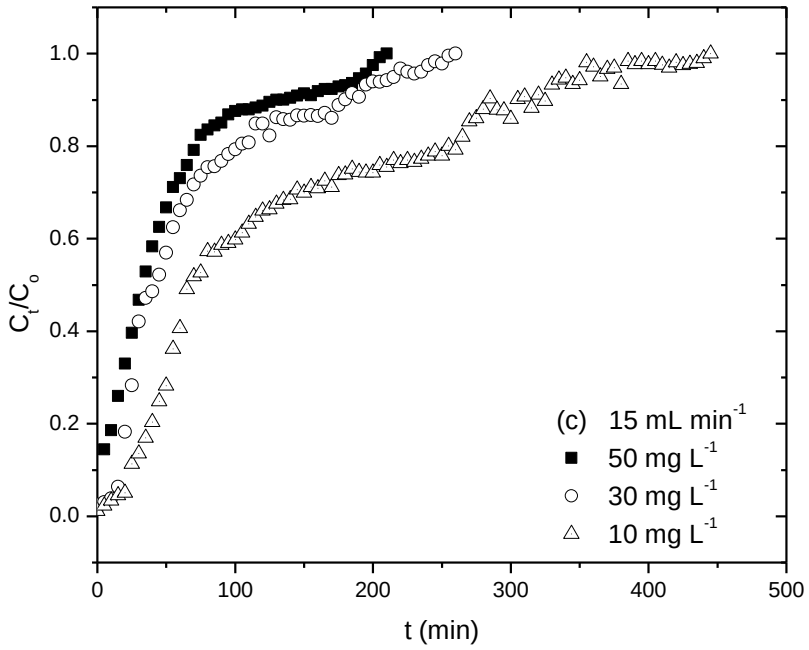

Figure 3: Breakthrough curves for the adsorption of MB onto raw rice husk: (a) Q= 5 mL min^{-1}, (b) Q=10 mL min^{-1} and (c) Q=15 mL min^{-1} (■ 50 mg L^{-1}, ○ 30 mg L^{-1} and Δ 50 mg L^{-1}).

Table II: Experimental conditions and results for the fixed bed adsorption of MB onto raw rice husk.

Run	Q (mL min^{-1})	C_o (mg L^{-1})	t_b (min)*	t_e (min)*	Z_m (cm)*	V_{eff} (mL)*	q_{eq} (mg g^{-1})*	R (%)*
1	5 (–1)	10 (–1)	109	552	20.1	3275	1.55	54.01
2	5 (–1)	30 (0)	50	330	20.8	1900	2.34	48.22
3	5 (–1)	50 (+1)	19	275	23.3	1650	3.52	48.72
4	10 (0)	10 (–1)	36	410	22.8	4975	1.27	29.25
5	10 (0)	30 (0)	26	260	22.5	3025	2.44	30.91
6	10 (0)	50 (+1)	4	150	24.4	2325	2.69	26.58
7	15 (+1)	10 (–1)	25	370	23.3	6790	1.73	29.39
8	15 (+1)	30 (0)	13	215	23.5	3940	2.58	25.09
9	15 (+1)	50 (+1)	2	190	24.8	3190	2.76	19.95

From Figure 3 and Table II it is possible to determine some important trends: (1) when the flow rate (Q) and/or the initial MB concentration (C_0)

increases, the breakthrough and exhaustion times tends to decrease; (2) the lower Z_m value and the higher removal percentage (R) were found at flow rate of 5 mL min^{-1} and initial MB concentration of 10 mg L^{-1}; (3) the high value for the maximum capacity of the column (q_{eq}) was found for the low volume of treated effluent (V_{eff}). All cited facts are directly related with the mass transfer stability during the experiment. At lower flow rates, the residence time is higher. This provides a more stable and continuous mass transfer of MB onto the raw rice husk. The other important aspect is the role of MB initial concentration. Due to the higher concentration, the mass transfer gradient is high. This leads to a high value of maximum adsorption capacity. Similar trends were reported by Han et al. (2007) in the adsorption of methylene blue onto raw rice husk.

Determination of the optimal adsorption condition

RSM was applied aiming to determine the optimal adsorption conditions for the selected responses (t_b, Z_m, q_{eq}), as a function of the flow rate and initial MB concentration. Also, RSM was used to obtain predictive equations which can represent the responses as a function of the independent variables. The experimental conditions (coded and real values) and the respective responses are represented in Table II. For each response, a statistical polynomial model, equation 9, was applied to represent the response as a function of the independent variables (Myers and Montgomery, 2002):

$$Y = \mu + \alpha C_0 + \beta C_0^2 + \gamma Q + \delta Q^2 + \varepsilon C_0 Q \quad (9)$$

where, Y is the response (t_b, Z_m, q_{eq}), α, β, γ, δ and ε are the regression coefficients.

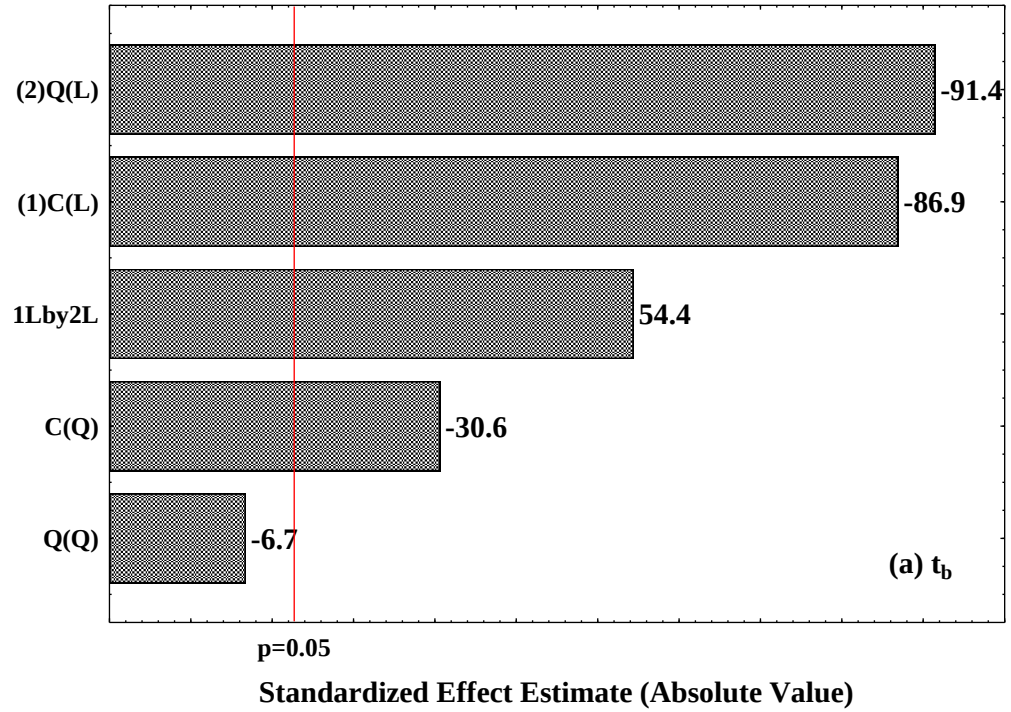
(2)Q(L)
-91.4
(1)C(L)
-86.9
1Lby2L
54.4
C(Q)
-30.6
Q(Q)
-6.7
(a) t_b
p=0.05
Standardized Effect Estimate (Absolute Value)

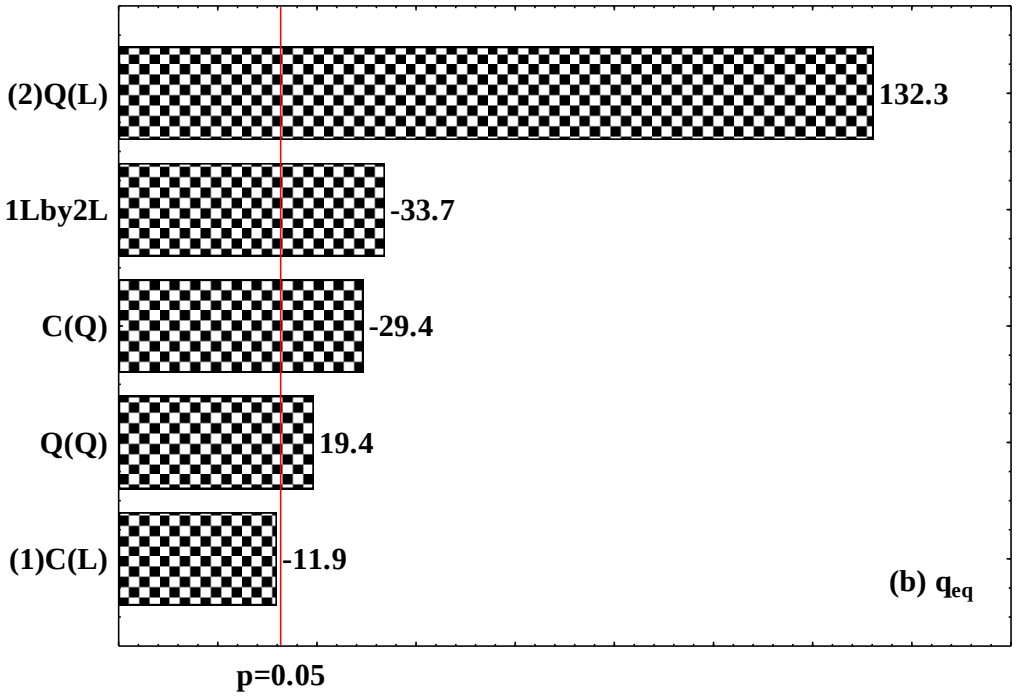
(2)Q(L)
132.3
1Lby2L
-33.7
C(Q)
-29.4
Q(Q)
19.4
(1)C(L)
-11.9
(b) q_{eq}
p=0.05
Standardized Effect Estimate (Absolute Value)

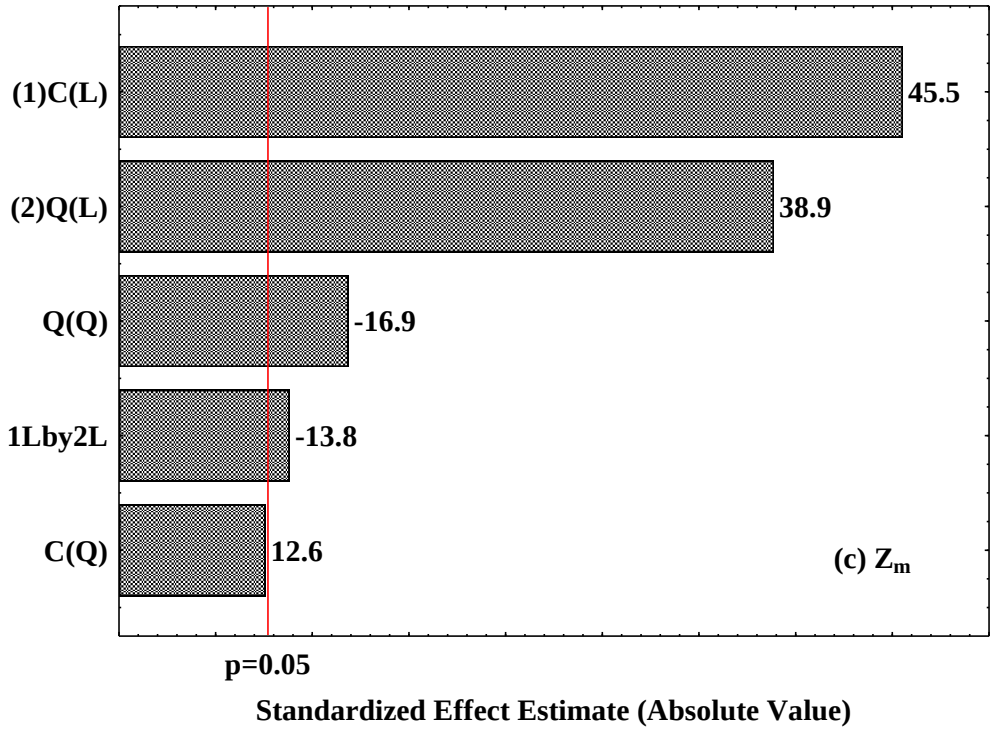

Figure 4: Pareto charts for the responses: (a) breakthrough time, (b) maximum adsorption capacity and (c) length of mass transfer zone.

The significance of the linear, quadratic and interaction effects on each response was evaluated through Pareto charts, as shown in Figure 4. The results revealed that the majority of linear, quadratic and interaction effects were significant for the t_b, Z_m, q_{eq} responses ($p<0.05$). The non significant effects were removed from the analysis. The statistical polynomial equation should be significant, predictive and reliable for a satisfactory representation of the experimental data (Myers and Montgomery, 2002). The high values of the coefficient of determination ($R^2>0.96$) showed that the polynomial quadratic models were significant (Table III). The Fischer's *F* test was used, and all the *F* values for each model were higher than the standard *F*, showing that the models were predictive (Table III). Lastly, the reliability of the model was evaluated by the comparison of the predicted and experimental values, as presented in Figure 5. It can be seen in Figure 5, that the models can predict satisfactorily the experimental data. Based on the abovementioned statistical evaluation, it can be affirmed that the polynomial quadratic models were significant, predictive and reliable. In this way, t_b, Z_m and q_{eq} can be represented by these models.

Table III: Regression coefficients and statistical parameters of the quadratic models for the responses, breakthrough time, maximum adsorption capacity of the column and length of mass transfer zone.

Response	Regression coefficients						Statistical parameters		
	μ	A	β	γ	δ	ε	R^2	F_{calc}	$F_{standard}$
t_b (min)	32.05	–23.90	–7.53	–25.15	–1.66	17.85	0.9725	55.85	3.11
q_{eq} (mg g^{-1})	2.26	–0.06	0.29	0.73	–0.19	–0.22	0.9621	53.36	
Z_m (cm)	22.68	1.25	–0.62	1.07	0.83	–0.45	0.9879	89.93	

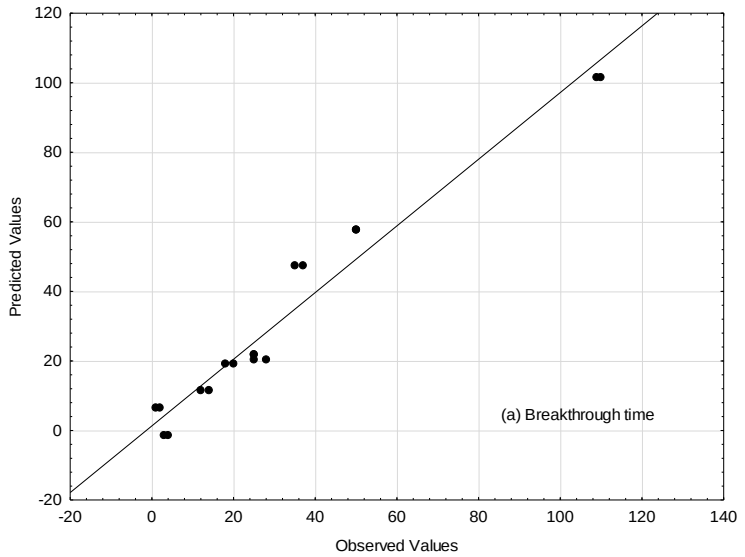

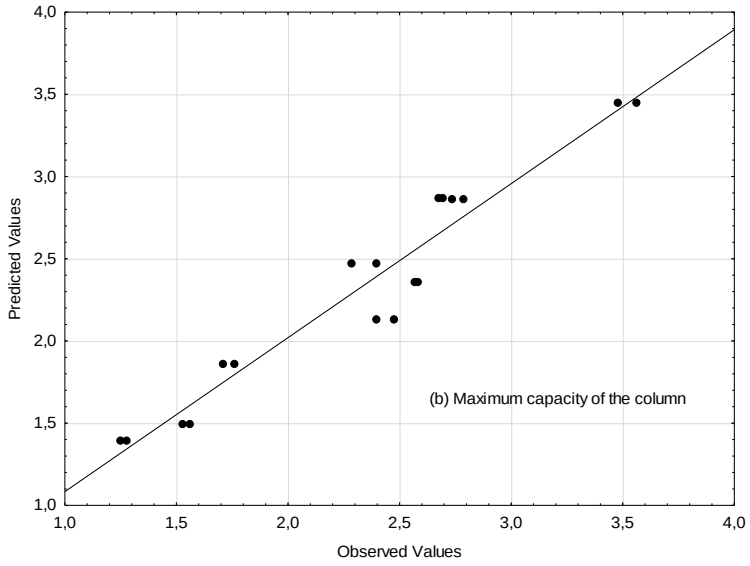

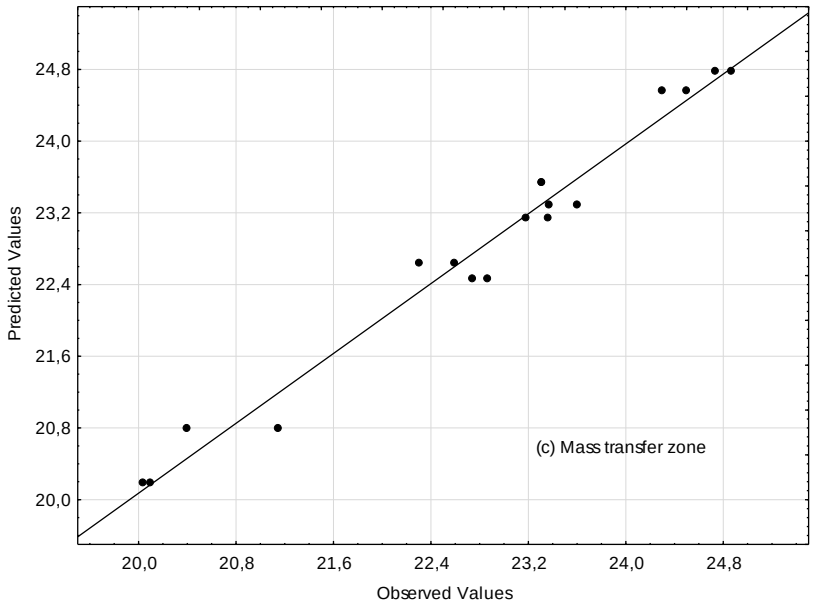

Figure 5: Predicted versus observed values for (a) breakthrough time, (b) maximum adsorption capacity and (c) length of mass transfer zone.

Since the models are significant, predictive and reliable, response surfaces were constructed to represent t_b, Z_m and q_{eq} as a function of Q and C_0. These surfaces are presented in Figure 6. Based on Figure 6 and Equation 9, an optimal condition was obtained for the fixed bed adsorption of MB. This condition occurs when t_b and q_{eq} are maximized and Z_m is minimized. It was verified that under the studied range, any point can satisfies simultaneously these conditions. Since the bed operation is generally performed until t_b, and Z_m is dependent of t_b, these two responses were considered the most relevant. In this sense, the optimal bed performance was: flow rate of 5 mL min^{-1} and initial MB concentration of 10 mg L^{-1}. Under these conditions the breakthrough time was 109 min, the length of mass transfer zone was 20.1 cm and the maximum capacity of the column was 1.55 mg g^{-1}.

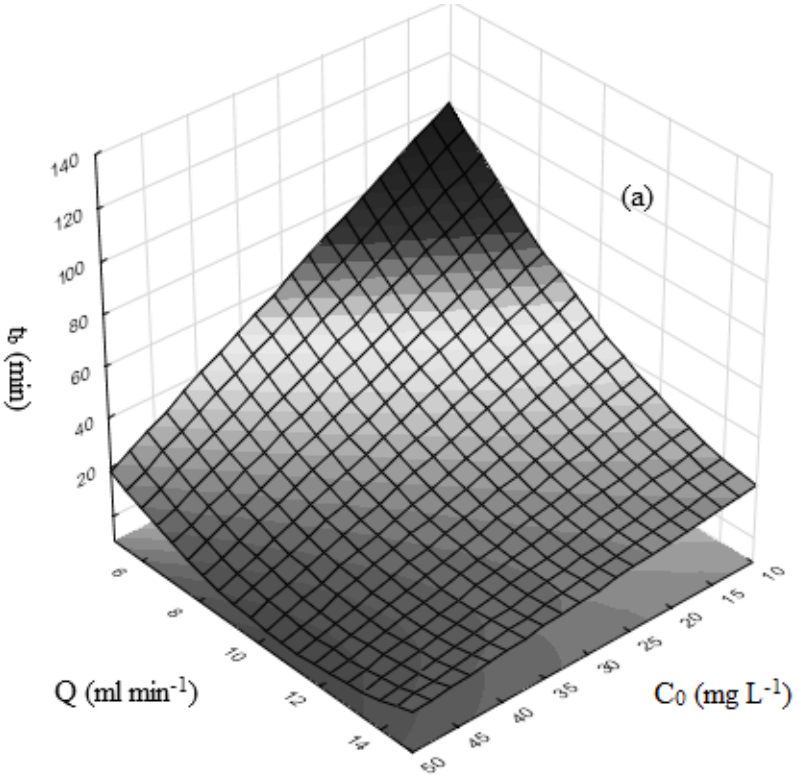
(a)
tb (min)
140
120
100
80
60
40
20
Q (ml min-1)
6
8
10
12
14
C0 (mg L-1)
10
15
20
25
30
35
40
45
50

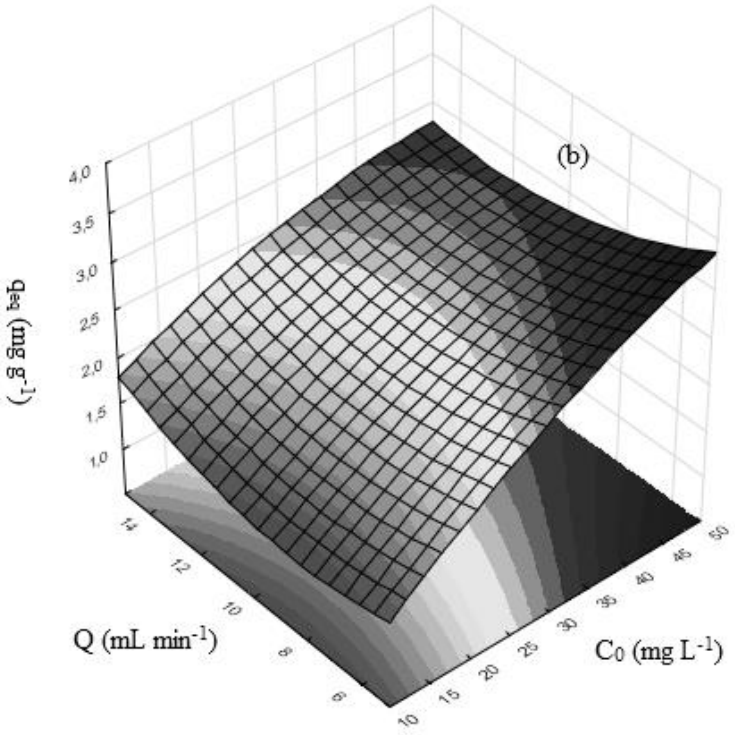
(b)
qeq (mg g-1)
4,0
3,5
3,0
2,5
2,0
1,5
1,0
Q (mL min-1)
14
12
10
8
6
C0 (mg L-1)
10
15
20
25
30
35
40
45
50

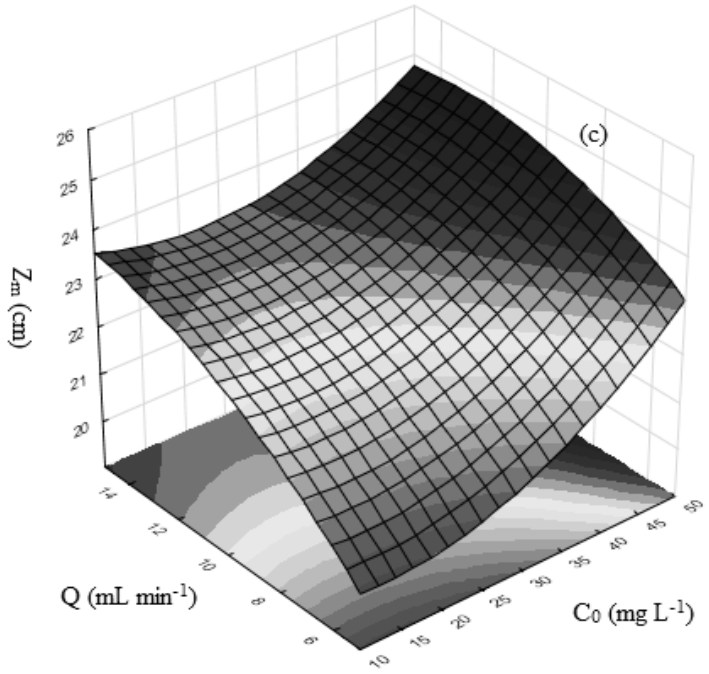

Figure 6: Response surfaces for (a) breakthrough time, (b) maximum adsorption capacity and (c) length of mass transfer zone as functions of the independent variables.

Effect of rice husk surface modification on the bed performance

In the optimal condition (obtained using raw rice husk), new experiments were performed with raw rice husk, UA–rice husk, SCO_2–rice husk and NaOH–rice husk as adsorbents, to investigate the effect of surface modifications on the bed performance. These results are presented in Table IV and Figure 7.

It was verified in Figure 7 that all modifications on the rice husk surface caused improvements on the breakthrough curves. The more pronounced improvement was found when NaOH–rice husk was used. In this case, the breakthrough time increased from 109 to 385 min, the length of mass transfer zone decreased from 20.1 to 9.3 cm, the maximum capacity of the column increased from 1.55 to 2.15 mg g^{-1} and the removal percentage increased 15% (compared with raw–rice husk) (Table IV). The three possible explanations are: (1) the surface modifications provided new available sites for MB adsorption; (2) the surface modifications caused ruptures on the rice husk, and opened new

possible paths for the influent flow, thus reaching new places for adsorption; (3) the rice husk porosity was changed, therefore, the influent flow pattern and the mass transfer rate were modified.

In general, it can be affirmed that all the surface modifications were favorable for MB adsorption in fixed bed. Due these modifications, the bed performance was largely improved as presented in Figure 7 and Table IV.

Table IV: Experimental fixed bed parameters for MB adsorption on raw rice husk, UA–rice husk, SCO_2–rice husk and NaOH–rice husk.

Adsorbent	t_b (min)*	t_e (min)*	Z_m (cm)*	V_{eff} (mL)*	q_{eq} (mg g^{-1})*	R (%)*
Raw rice husk	109	552	20.1	3275	1.55	54.01
UA–rice husk	240	350	7.9	2125	1.30	67.20
SCO_2–rice husk	155	425	15.9	2575	1.20	51.10
NaOH–rice husk	385	615	9.3	3350	2.15	70.01

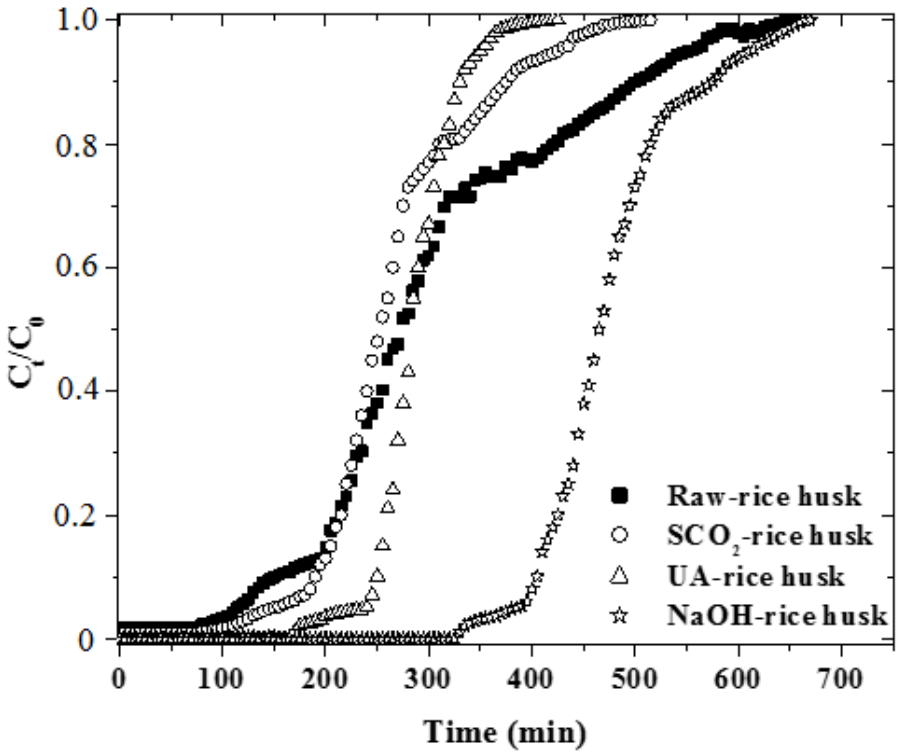

Figure 7: Effect of the rice husk surface modifications on the breakthrough curves (■ raw rice husk, ☆ NaOH–rice husk, Δ UA–rice husk and ○ SCO_2–rice husk).

Application of dynamic models

The experimental curves in Figure 7 were fitted with the Bed Depth Service Time (BDST), Thomas and Yoon–Nelson dynamic models, in order to better understand the fixed bed adsorption of MB. The results are presented in Table V.

Based on the high values of the coefficient of determination (R^2>0.98) and in the low values of the sum of squared errors (SSE<0.28), it can be affirmed that all the dynamic models were able to represent the breakthrough curves. The modeled parameters were in agreement with the experimental curves and were physically consistent. The theoretical and experimental q_{eq} values were similar for all adsorbents. In the same way, the experimental and theoretical τ values were in accordance.

Table V: Parameters of the dynamic models in the fixed bed adsorption of MB on raw rice husk, UA–rice husk, SCO_2–rice husk and NaOH–rice husk.

Models	Adsorbents			
	Raw–rice husk	UA–rice husk	SCO_2–rice husk	NaOH–rice husk
Thomas				
$k_{th}\times10^3$ (L mg^{-1} min^{-1})	1.42	5.18	2.60	2.91
q_{eq} (mg g^{-1})	1.30	1.30	1.17	2.13
$q_{eq\ (exp)}$(mg g^{-1})	1.55	1.30	1.20	2.15
Yoon–Nelson				
K_{YN} (min^{-1})	0.0141	0.0518	0.0260	0.0291
τ (min)	285	284	257	468
τ_{exp} (min)	275	282	252	465
BDST				
$K\times10^3$ (L mg^{-1} min^{-1})	1.42	5.18	2.60	2.91

No (mg L^{-1})	115.8	115.3	104.1	189.4
Statistical parameters				
R^2	0.9853	0.9988	0.9930	0.9975
SSE	0.2748	0.0180	0.1246	0.0514

Conclusion

The fixed bed adsorption of Methylene Blue dye (MB) on surface modified rice husk was investigated. Based on the characterization techniques, it was found that all the employed modifications caused changes on the rice husk surface. The application of RSM indicated that the optimal bed performance, using raw rice husk, was found at flow rate of 5 mL min^{-1} and initial MB concentration of 10 mg L^{-1}. Under these conditions the breakthrough time was 109 min, the length of mass transfer zone was 20.1 cm and the maximum capacity of the column was 1.55 mg g^{-1}. When the surface modified adsorbents were applied, the bed performance was significantly improved. The breakthrough times were 109, 240, 155 and 385 min, for raw rice husk, UA–rice husk, SCO_2–rice husk and NaOH–rice husk, respectively. The length of mass transfer zone was 20.1, 7.9, 15.9 and 9.3 cm for raw rice husk, UA–rice husk, SCO_2–rice husk and NaOH–rice husk, respectively. The dynamic models were able to fit the adsorption data and provided physically consistent parameters. In summary, this work demonstrated that the surface modifications on the rice husk were favorable to improve the bed performance in the MB adsorption.

Acknowledgments

The authors would like to thank CAPES (Coordination for the Improvement of Higher Education Personnel) and CNPq (National Council for Scientific and Technological Development) for the financial support.

References

Chakraborty, S., Chowdhury, S., Saha, P. D. (2011). Adsorption of Crystal Violet from aqueous solution onto NaOH–modified rice husk, *Carbohydr. Polym.* 86, 1533–1541.

Dobre, T., Pârvulescu, O. C., Jacquement A. (2016). Adsorption and Thermal Desorption of Volatile Organic Compounds in a Fixed Bed – Experimental and Modeling, *Chem. Eng. Commun*. In press, doi: 10.1080/00986445.2016.1151417.

Dod, R., Banerjee, G., Saini, D.R. (2015). Removal of methylene blue (MB) dye from water environment by processed Jowar Stalk [*Sorghum bicolor (L.) Moench*] adsorbent, *Clean Technol. Environ. Pol*. 17, 2349–2359.

Dotto, G. L., Costa, J. A. V., Pinto, L. A. A. (2013). Kinetic studies on the biosorption of phenol by nanoparticles from *Spirulina* sp. LEB 18, *J. Environ. Chem. Eng.* 1, 1137–1143.

Dotto, G. L., Cunha, J. M., Calgaro, C. O., Tanabe, E. H., Bertuol, D. A. (2015b). Surface modification of chitin using ultrasound–assisted and supercritical CO_2 technologies for cobalt adsorption, *J. Hazard. Mater.* 295, 29–36.

Dotto, G. L., Santos, J. M. N., Rosa, R., Pinto, L. A. A., Pavan, F. A., Lima, E. C. (2015a). Fixed bed adsorption of Methylene Blue by ultrasonic surface modified chitin supported on sand, *Chem. Eng. Res. Des.* 100, 302–310.

FAO (2015). FAO Rice Market Monitor. FAO 28, 1–27.

Ginimuge, P. R., and Jyothi, S. D. (2010). Methylene Blue: Revisited, *Clinic. Pharmacol*. 26, 517–520.

Goldstein, J. I., Newbury, D. E., Echil, P., Joy, D. C., Romig Jr., A. D., Lyman, C. E., Fiori, C., Lifshin, E. (1992). *Scanning Electron Microscopy and X–ray Microanalysis*. Plenum Press, New York.

Guo, C., Kong, Q., Gao, J., Ji, Q., Xia, Y. (2011). Removal of methylene blue dye from simulated wastewater by alginic acid fiber as adsorbent: Equilibrium, kinetic, and thermodynamic studies, *Can. J. Chem. Eng*., 89, 1545–1553.

Gupta, V. K., and Suhas, I. (2009). Application of low–cost adsorbents for dye removal: A review, *J. Environ. Manage*., 90, 2313–2342.

Han, R., Wang, Y., Yu, W., Zou, W., Shie, J., Liu, H. (2007). Biosorption of methylene blue from aqueous solution by rice husk in a fixed–bed column, *J. Hazard. Mater.*, 141, 713–718.

Hutchins, R.A. (1973). New method simplifies design of activated carbon systems, *Amer. J. Chem. Eng*. 80, 133–138.

Kant, R. (2013). Textile dyeing industry an environmental hazard, *Nat. Sci.* 4, 22–26.

Lin, L. Zhai, S. R., Xiao, Z. Y., Song, Y., An, Q. D., Song, X. W. (2013). Dye adsorption of mesoporous activated carbons produced from NaOH–pretreated rice husks, *Bioresour. Technol.* 136, 437–443.

Myers, R. H., Montgomery, D. C. (2002). *Response Surface Methodology: Process and Product Optimization Using Designed Experiments*. John Wiley & Sons, New York.

Silverstein, R. M., Webster, F. X., Kiemle, J. D. (2007). *Spectrometric Identification of Organic Compounds.* John Wiley & Sons, New York.

Soltani, N., Bahrami, A., González, L. A. (2014). Review on the physicochemical treatments of rice husk for production of advanced materials, *Chem. Eng. J.* 264, 899–935.

Suzuki, M. (1990). *Adsorption Engineering.* Kodansha, Tokyo.

Tanabe, E. H., Schlemmer, D. F., Aguiar, M. L., Dotto, G. L., Bertuol, D. A. (2016). Recovery of valuable materials from spent NIMH batteries using spouted bed elutriation, *J. Environ. Manage.* 171, 177–183.

Thakur, K. V. (2014). *Lignocellulosic Polymer Composites: Processing, Characterization and Properties*. Wiley and Scrivener, Salem and Massachusetts.

Thomas, H.C. (1944). Heterogeneous ion exchange in a flowing system, *J. Amer. Chem. Soc*. 66, 1466–1664.

Weng, C., Lin, Y., Tseng, T. (2009). Removal of methylene blue from aqueous solution by adsorption onto pineapple leaf powder, *J. Mol. Liq*. 170, 417–424.

Yin, C. Y., Aroua, M. K., Daud, W. M. A. W. (2009). Fixed–bed adsorption of metal ions from aqueous solution on polyethyleneimine–impregnated palm shell activated carbon, *Chem. Eng. J.* 148, 8–14.

Yoon, Y. H., Nelson, J. H. (1984). Application of gas adsorption kinetics: Part 1: A theoretical model for respirator cartridge service time*, Amer. Ind. Hyg. Assoc*. *J.* 45, 509–516.

5 CONCLUSÃO

Neste trabalho verificou-se que as modificações aplicadas à superfície da casca de arroz, melhoraram o seu potencial como adsorvente do corante azul de metileno. As caracterizações realizadas (FTIR, DRX, MEV e EDS) demonstraram que uma parte da fração orgânica foi exposta e que a fração de sílica foi removida da superfície indicando a criação de novos sítios para adsorção. No estudo em batelada, foi possível concluir que a casca de arroz modificada com NaOH apresentou resultado superior em comparação aos outros adsorventes em relação a capacidade de adsorção ($q_{NaoH=}$ 65,0 mg g^{-1},q_{UA}= 58,7 mg g^{-1},q_{SCO2}= 56,4 mg g^{-1},$q_{in\ natura}$= 52,2 mg g^{-1}). Em conjunto com as modificações de superfície foi constato que o aumento da temperatura promove o aumento da capacidade de adsorção. O estudo termodinâmico mostrou que a adsorção foi, espontânea, favorável, endotérmica e controlada pela entropia.

O uso da casca de arroz e suas modificações na adsorção em leito fixo foram também investigados. A otimização experimental conduzida indicou que a condição ótima de operação foi com uma vazão de 5 mL min^{-1} e uma concentração inicial de 10 mg L^{-1} de azul de metileno, para a casca de arroz *in natura*, resultando em um t_r= 109 min, z_m= 20,1 cm e q_{eq}= 1,55 mg g^{-1}. Quando aplicado para os outros adsorventes foram encontrados um tempo de ruptura de 240, 155 e 385 min e uma zona de transferência de massa de 7,9, 15,9 e 9,3 cm, para casca de arroz NaOH, SCO_2, UA respectivamente, indicando que as técnicas de modificação de superfície melhoraram o desempenho geral do leito.

Em geral pode-se concluir que as modificações realizadas na casca de arroz promoveram benefícios em relação ao seu potencial adsorvente. No estudo em batelada verificou-se que as capacidades de adsorção foram aumentadas. No estudo em leito fixo verificou-se que os parâmetros operacionais foram melhorados, melhorando assim o desempenho do leito.

Sugestões para trabalhos futuros

- Investigar a cinética de adsorção e o mecanismo de transferência de massa para os adsorventes desenvolvidos neste trabalho;
- Aplicar um planejamento experimental no processo de modificação da casca de arroz com hidróxido de sódio, levando em consideração como variáveis à concentração do hidróxido de sódio, a massa de casca e o tempo de agitação;
- Investigar a influência das modificações para adsorção de outros corantes.

6 REFERÊNCIAS

ANASTOPOULOS, I.; KYZAS, G. Z. Are the thermodynamic parameters correctly estimated in liquid-phase adsorption phenomena? **Journal of Molecular Liquids**, v. 218, p. 174–185, 2016.

Asfour, H.M., Fadali, O.A., Nassar, M.M., El-Geundi, M.S. Equilibrium studies on adsorption of basic dyes on hardwood. **Journal of Chemical Technology and Biotechnology.** 35A, 21–27, 1985.

Aziz, A., Ouali, M.S., Elandaloussi, E.H., Charles De Menorval, L., Lindheimer, M.. Chemically modified olive stone: a low-cost sorbent for heavy metals and basic dyes removal from aqueous solutions. **Journal of Hazardous. Material.** 163 (1), 441-447, 2009.

BRENNER, H. **Adsorption Calculations and Modelling**. 1st, 1994.

CONAB. AACOMPANHAMENTO DA SAFRA BRASILEIRA grãos. **Monitoramento Agrícola**, v. 2, n. 9, p. 1–104, 2016.

DOD, R.; BANERJEE, G.; SAINI, D. R. Removal of methylene blue (MB) dye from water environment by processed Jowar Stalk [Sorghum bicolor (L.) Moench] adsorbent. **Clean Technologies and Environmental Policy**, v. 17, n. 8, p. 2349–2359, 2015.

DOTTO, G. L. et al. Adsorption of Methylene Blue by ultrasonic surface modified chitin. **Journal of colloid and interface science**, v. 446, p. 133–140, 2015.

DOTTO, G. L. et al. Comparison between Brazilian agro-wastes and activated carbon as adsorbents to remove Ni(II) from aqueous solutions. **Water Science and Technology**, v. 73, n. 11, p. 2713–2721, 2016.

DOTTO, G. L.; PINTO, L. A. A. Adsorption of food dyes acid blue 9 and food yellow 3 onto chitosan: Stirring rate effect in kinetics and mechanism. **Journal of Hazardous Materials**, v. 187, n. 1-3, p. 164–170, 2011.

FAO. **FAO Rice Market Monitor.** FAO 28, 1–27, 2015.

GEANKOPLIS, C. J. **Transport Processes and Unit Operations,** Prentice-Hall International, 1993.

FRANCO, D. S. P., MARTINS, J. M., RODRIGUES, L. M., E ALMEIDA, A. R. F. Análise do Processo de Secagem de Sementes de Mamão Utilizado

como Biomassa Adsorvente no Tratamento de Efluentes. **Revista. de Ciências. Exatas,** RJ, EDUR, v. 27/31, n. 2, p. 44-59, 2012

GUPTA, V. K.; SUHAS. Application of low-cost adsorbents for dye removal - A review. **Journal of Environmental Management**, v. 90, n. 8, p. 2313–2342, 2009.

HUTCHINS, R.A. New method simplifies design of activated carbon systems**, American Journal of Chemical Engineering**. 80, 133–138, 1973.~

IMRAN ALI, M. A. Low cost adsorbents for the removal of organic polutans from wastewater. **Enviromental Managment**, v. 113, p. 170–183, 2012.

Kannan, N., Sundaram, M.M.**.** Kinetics and mechanism of removal of methylene blue by adsorption on various carbons – a comparative study**. Dyes Pigments** 51, 25–40, 2001**.**

KANT, R. Textile dyeing industry an environmental hazard. **Natural Science**, v. 4, n. 1, p. 22–26, 2013.

KHALFAOUI, M. et al. New theoretical expressions for the five adsorption type isotherms classified by BET based on statistical physics treatment. **Journal of Colloid and Interface Science**, v. 263, n. 2, p. 350–356, 2003.

LANGMUIR, I. The Adsorption of Gases on Plane Surfaces of Glass, Mica and Platinum. **Journal of the American Chemical Society**, v. 40, n. 9, p. 1361–1403, 1918.

MCCABE, W. L.; SMITH, J. C.; HARRIOTT, P. **Unit Operations of Chemical Engineering**, 1993.

McKay, G., Porter, J.F., Prasad, G.R. The removal of dye colors from aqueous solutions by adsorption on low-cost material. **Water, Air, & Soil Pollution.** 114, 423-438, 1999.

Nasser, M.M., Hamoda, M.F., Radwan, G.H. Utilization of palm-fruit bunch particles for the adsorption of dye stuff wastes. **Adsorption Science and Technology**. 13, 1-6, 1996.

Nawar, S.S., Doma, H.S. Removal of dyes from effluents using low-cost agricultural by-products. **Science of the Total Environment.** 79, 271-279, 1989.

RICHARDSON, J. F.; HARKER, J. H. Coulson & Richardson's Chemical Engineering: Volume 2. **Design**, v. 40, p. 9823, 2001.

RUTHVEN M. DOUGLAS. **Principles of Adsorption and Adsorption Processes**. [s.l.] John Wiley & Sons, 1984.

SOLTANI, N.; BAHRAMI, A.; GONZÁLEZ, L. A. Review on the physicochemical treatments of rice husk for productionof advanced materials. **Chemical Engineering Journal**, v. 264, p. 899–935, 2014.

SUGASHINI, S.; BEGUM, K. M. M. S. Performance of ozone treated rice husk carbon (OTRHC) for continuous adsorption of Cr (VI) ions from synthetic effluent. **Journal of Environmental Chemical Engineering**, v. 1, n. 1-2, p. 79–85, 2013.

SUZUKI, M. **Adsorption Engineering**. Kodansha, Tokyo, 1st, 1990..

THAKUR, V. K. **Lignocellulosic Polymer Composites: Processing, Characterization and Proprieties**. v. 1, 2014

THOMAS, H.C. Heterogeneous ion exchange in a flowing system, **Journal of American Chemical Society. Soc**. 66, 1466–1664, 1944.

WANG, Y. et al. Application of longan shell as non-conventional low-cost adsorbent for the removal of cationic dye from aqueous solution. **Spectrochimica Acta Part A: Molecular and Biomolecular Spectroscopy**, v. 159, p. 254–261, 2016.

YAGUB, M. T. et al. Dye and its removal from aqueous solution by adsorption: A review. **Advances in Colloid and Interface Science**, v. 209, p. 172–184, 2014.

YANG, R. T. **Adsorbents Adsorbents : Fundamentals and Applications**. [s.l: s.n.].

YOON, Y. H., NELSON, J. H. Application of gas adsorption kinetics: Part 1: A theoretical model for respirator cartridge service time, **American Industrial Hygiene Association Journal**. 45, 509–516, 1984.